# Tribology of Atomically Smooth Surfaces

by

Tae Hun Kang

S.B., Mechanical Engineering
Massachusetts Institute of Technology, June 1989

Submitted to the Department of Mechanical Engineering
in Partial Fulfillment of the Requirements for the Degree of

MASTER OF SCIENCE IN MECHANICAL ENGINEERING

at the

MASSACHUSETTS INSTITUTE OF TECHNOLOGY

December 1991



Signature of Author: _____
Department of Mechanical Engineering
December 18, 1991

Certified by: _____
Nam P. Suh
Professor, Department of Mechanical Engineering
Thesis Supervisor

Accepted by: _____
Ain A. Sonin
Chairman, Department Graduate Committee

TRIBOLOGY OF ATOMICALLY SMOOTH SURFACES

by

TAE HUN KANG

Submitted to the Department of Mechanical Engineering
on December 19, 1991 in partial fulfillment of the
requirements for the Degree of Master of Science in
Mechanical Engineering

## ABSTRACT

Friction is the manifestation of nonmechanical (adhesion) and mechanical (asperity deformation and plowing by wear particles and by hard asperities) interactions at the sliding interface. During the past decade, plowing by wear particles and by hard asperities has been shown to be the dominant mechanism of friction in many situations. The purpose of this investigation was to better understand the fundamental causes of friction. The approach was to separate nonmechanical from mechanical interactions by using "atomically smooth" surfaces.

Diverse experiments have indicated that for crystalline solids, both macro- and micro-frictional behavior is dominated by mechanical interactions at and below the sliding interface. This was evident from two observations: (1) Similar values of friction coefficients ($\sim 0.1$) were obtained in experiments conducted in air for dry sliding of various atomically smooth, hard, and flat surfaces under relatively low loads ($\sim 10^{-2}$ N, surface and subsurface damage detected by chemical etching of the surfaces) as well as under extremely low loads ($\sim 10^{-4}$ N, undetectable surface damage). Even atomic scale roughness (0.1 nm) was large enough to cause mechanical interactions in the form of dislocation generation and motion; (2) Effects of adsorbed molecules were negligible on friction. Vacuum ($10^{-5}$ Torr) and vacuum+heat (400° C) had no effect on the value of friction coefficients.

The experiments have also indicated that the minimum friction and wear may be achieved by resisting crack nucleation and propagation and by confining the interaction at asperity contacts to smooth noncrystalline materials that have good elastic behavior (i.e., no viscoelastic or anelastic behavior). Furthermore, the elastic behavior should be confined to a very thin layer on top of a hard substrate in order to minimize the energy dissipation due to unavoidable anelastic and viscoelastic effects. When such a material is prepared so as to have atomic scale or micron scale surface roughness, the energy dissipation, hence the friction, should be extremely small.

Thesis Supervisor: Dr. Nam P. Suh

Title: Professor of Mechanical Engineering

## Acknowledgements

I would like to extend my sincere gratitude to my mentor, professor Nam P. Suh, for being patient and caring enough to tolerate two years of "blunders" on my part. The knowledge that I gained from him was not only in science but also about life in general. I will always be grateful and indebted to him.

I would also like to thank Dr. Nannaji Saka for many insights and help during the past two years. Mr. Fred Cote also has my gratitude for his help in building the friction testing apparatus used in this investigation. Mr. Joe Davis at Pilgrim Mixing Company, was very gracious in allowing me access to his factory. I am also grateful to Dr. Dae Eun Kim for all his help.

Most of all, I would like to express my love and respect to my parents, my brother, my sister, my brother-in-law, and finally to God in Heaven for giving me the opportunity to study in a place like M.I.T. Their love and support in my walk through M.I.T. life has made it possible for me to complete this study.

*"The quality of a person's life is in direct proportion to their commitment to excellence, regardless of their chosen field of endeavor."*

*"Wisdom is a shelter as money is a shelter, but the advantage of knowledge is this: that wisdom preserves the life of its possessor."*

*Ecclesiastes 7:12*

## Table of Contents


| | Page No. |
|---|---|
| **Title Page** | 1 |
| **Abstract** | 2 |
| **Acknowledgments** | 3 |
| **Table of Contents** | 4 |
| **List of Figures** | 6 |
| **List of Tables** | 8 |
| **Chapter 1 Introduction** | 9 |
| 1.1 General Introduction | 9 |
| 1.2 Microscopic Investigations Into Friction | 15 |
| 1.3 Research Issues | 17 |
| 1.4 Impact of the Research | 20 |
| 1.5 Outline of the Thesis | 20 |
| 1.6 References | 22 |
| **Chapter 2 Friction Experiments On Atomically Smooth Surfaces** | 25 |
| 2.1 Introduction | 25 |
| 2.2 Apparatus | 26 |
| 2.3 Materials | 33 |
| 2.4 Experiments in Ambient and in Clean Room | 33 |
| 2.4.1 Results from Ambient and Clean Room Experiments | 34 |
| 2.4.2 Conclusions from Ambient and Clean Room Experiments | 40 |
| 2.5 Experiments in Vacuum | 45 |
| 2.5.1 Preparation for the Experiment | 45 |
| 2.5.2 Experimental Procedure | 45 |
| 2.5.3 Results from Vacuum Experiments | 46 |
| 2.5.4 Discussion and Conclusions from Vacuum Experiments | 52 |
| 2.5.4.A Surface of Glasses | 52 |
| 2.5.4.B Surface Conditions of Si and SiC | 54 |
| 2.5.4.C Conclusions | 55 |
| 2.6 References | 59 |

Appendix I 60
**Chapter 3 Elastomers** 68
3.1 Introduction 68
3.2 The Dry Sliding Friction Mechanism of Rubber 69
3.3 Preparation of the Samples 70
3.4 Experimental procedure 70
3.5 Experimental Results 74
3.6 Discussion and Conclusions 74
3.7 References 84
Appendix I 85
**Chapter 4 Conclusions and Recommendations** 87
4.1 Conclusions 87
4.2 Recommendations 88

## List of Figures


| Figure No. | | Page No. |
|---|---|---|
| 1 | Friction Space | 12 |
| 2 | Typical Friction coefficient vs. Distance Slid Plot | 13 |
| 3 | Friction Plot - Effects Due to Removal of Wear Particles | 13 |
| 4 | Typical Undulated Surface | 14 |
| 5 | Friction Coefficient vs. Distance Slid: Copper on Copper, plain & Undulated Surfaces | 14 |
| 6 | Results from Investigations by Mate *et al* | 18 |
| 7 | SEM Photograph of the Wear Tracks of Si After Chemical Etching | 19 |
| 8 | Piezo-Friction Testing Apparatus - Photographs | 28 |
| 9 | Piezo-Friction Testing Apparatus - Schematic Drawing | 29 |
| 10 | RC Circuit | 30 |
| 11 | Response Plot of the RC Circuit | 32 |
| 12 | A Schematic response from the Chart Recorder | 32 |
| 13 | Optical Profilometer Printouts of $SiO_2$ | 36 |
| 14 | Optical Profilometer Printouts of SiC | 37 |
| 15 | Surface Contact Possibilities | 44 |
| 16 | Piezo-Friction Testing Apparatus - Modified | 47 |
| 17 | The "Solenoid Holder" | 48 |

| | | |
|---|---|---|
| 18 | Static Friction Coefficient vs. Temperature: Silica glass on Silica glass | 51 |
| 19 | Static Friction Coefficient vs. Temperature: Silica glass on SiC | 51 |
| 20 | Desorption from Glass Surfaces | 53 |
| 21 | Desorption from Si Surface | 56 |
| 22 | A Schematic Drawing of a Sulfur/Rubber Specimen | 71 |
| 23 | Destruction of Counter Surface by Hard particles Embedded During Polishing of Sulfur/Rubber Compounds | 71 |
| 24 | Durometer "Hardness" vs. % Sulfur | 72 |
| 25 | Reciprocating Friction Testing Apparatus | 73 |
| 26 | Steady State Friction Coefficient vs. % Sulfur: 20 and 50 mN Loads. | 75 |
| 27 | SEM Photographs of the Wear Tracks of Sulfur/Rubber | 76 |
| 28 | One possible Surface Damage Mode | 79 |
| 29 | Crack Initiation at the Surface | 82 |
| 30 | Theoretical Stress Distribution Produced by a Line Force on the Edge of a Semi-Infinite Elastic Plane; High Subsurface Stress Leading to Large Bulk Deformation | 82 |
| 31 | Very Thin Elastic Layer on Top of a Hard Substrate | 83 |
| 32. | "Whiskers" on the Surface of a Solid | 89 |
| I-1 | Adsorption Energy vs. Temperature | 66 |

## List of Tables


| Table No. | | Page No. |
|---|---|---|
| 1 | Average Roughness and Hardness of the Specimens | 35 |
| 2 | Friction Coefficients from Ambient Experiment | 38 |
| 3 | Friction Coefficients from Clean Room Experiment | 39 |
| 4 | Theoretically Predicted Value of an Increase in the Frictional Force - Elastic Contacts | 43 |
| 5 | Friction Coefficients from Vacuum (25° C) Experiment | 49 |
| 6 | Friction Coefficients from Vacuum + Heat (400° C) Experiment | 50 |
| I-1 | Adsorption Time for Several Adsorption Energies | 63 |

# Chapter 1

# Introduction

## 1.1 General Introduction

Tribology, the science of friction, lubrication, and wear, is unique among the learned disciplines in that it is an interdisciplinary subject that involves macro-to-micro scale phenomena. In the past, tribology problems have frequently been dealt with on an empirical basis and often from a single disciplinary point of view using over-simplified assumptions regarding geometric, physical, and chemical effects between sliding surfaces. Even among the experts in the field, there is an ongoing dispute regarding the inherent causes of friction.

Since the time of Amontons, scientists and engineers have observed three general facts regarding friction: (1) The frictional force is independent of the apparent area of contact; (2) The frictional force is independent of the sliding velocity; (3) The frictional force is directly proportional to the normal load. In order to explain these observations, Bowden and Tabor [1] developed the adhesion theory of friction during the 1940s. They correctly assumed that interactions at the contacting interface, due to surface roughness, occurred at a few localized regions known as asperity junctions. The apparent and real areas of contact are thus differentiated. They also assumed that at the asperity junctions, the sliding surfaces adhere to each other to form an adhesive bond due to atomic attraction. Friction then is the force required to shear either the softer material or the adhesive bond formed at the sliding interface. Since that time many workers have supported this theory using experimental data to show higher friction coefficients between identical materials in comparison with different materials. These

observations were explained in terms of greater adhesion in the case of identical materials [2-7].

From the adhesion theory, the theoretical value of the friction coefficient can be derived to be 0.17 [2]. Since this value is much smaller than the typical values observed under steady-state sliding conditions, many new concepts were introduced to explain the difference between the experimental and the theoretical values.

The most prominent and generally accepted explanation was that proposed by Rabinowicz [2], who stated that surface energy contribution must also be considered when calculating the real area of contact as shown below:

$$\pi r^2 = \frac{L}{H} + \frac{2\pi r}{\sin\theta}\frac{W_{ab}}{H} \qquad (1)$$

where r is the radius of each asperity contact, L the normal load on each asperity, H the hardness, $W_{ab}$ the energy of adhesion, and $\theta$ the slope of the asperity. The first term on the right-hand side represents the area of contact due to a flat indentor contacting a semi-infinite solid and the second term is the additional contact area due to the change in the interfacial area when adhesion occurs.

Upon careful examination of the equation, however, even this concept does not sufficiently explain the difference between the theoretical and the observed values of friction coefficients. An order of magnitude analysis of the equation shows that the additional increase in the real area of contact due to surface energy effect (second term) is actually much less than the originally calculated value of the real area of contact (first term), thus insufficient to

account for the large difference. Another reason for concern comes from the the questionable experimental values of surface energy [8]. Furthermore, since surfaces are always contaminated with at least a monolayer of molecules, some scientists doubt the formation of strong adhesive bonds necessary to justify the observed frictional force. Nevertheless, many scientists, even to this very day, explain friction strictly by the adhesion theory.

During the past decade, the researchers at M.I.T. have shown that contrary to the adhesion theory of friction, friction under normal engineering situations is primarily caused by "mechanical effects" such as asperity deformation and plowing by wear particles. The relative importance of the three components (plowing, asperity deformation, and adhesion) changes for a given pair of materials during the course of sliding [9]. The friction space concept was developed to graphically represent this theory as shown in Figure 1.

In a typical dry sliding experiment with polished metal surfaces, the friction coefficient starts at a low value (0.1 to 0.2) and steadily increases until a steady state value is reached (see Figure 2). The rise in friction coefficient is believed, by Suh and Sin [9], to be mainly due to plowing by wear particles. This belief was substantiated by two methods. First, the friction experiment was stopped once the friction coefficient reached a steady state value (high friction with respect to initial friction), and then wear particles were brushed away from the sliding interface. This resulted in a dramatic drop in the value of friction coefficient (see Figure 3). Second, the use of an undulated surface gives even more convincing evidence of dominant plowing effect. In this case grooves or "pockets" were made on one of the sliding surfaces in an attempt to entrap wear particles and thus prevent plowing (see Figure 4). Experiments have shown that undulated surfaces indeed maintain dry sliding friction coefficients between *identical* as well as *different* pairs of materials at a value as low as those observed under a boundary-lubricated case [10-11]. Figure 5 shows the results of copper sliding on copper for plain and undulated surfaces.

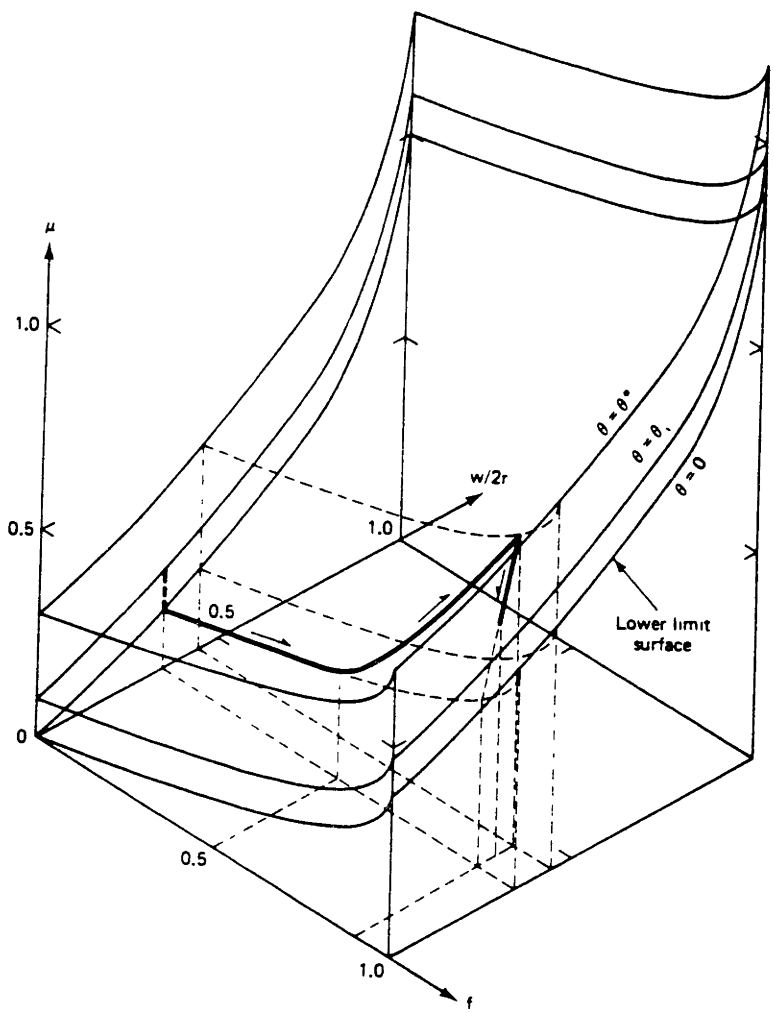


Figure 1: Friction Space [9]

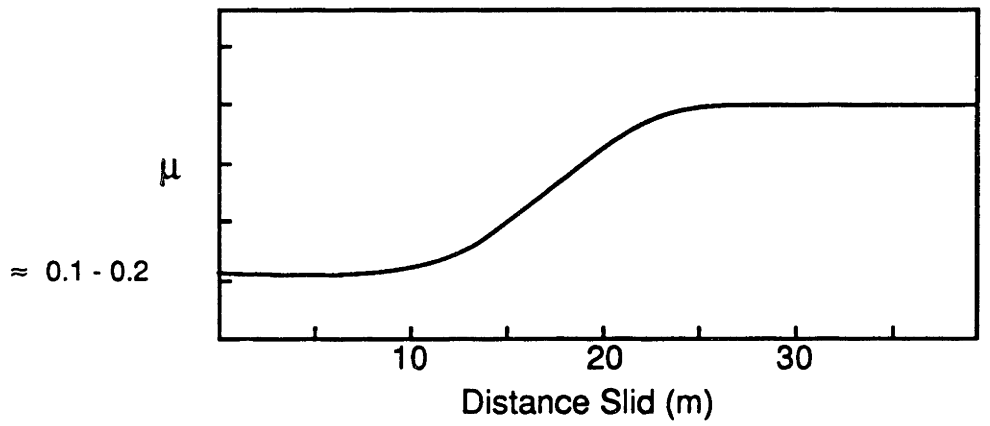


Figure 2: Typical Friction Coefficient vs. Distance Slid Plot

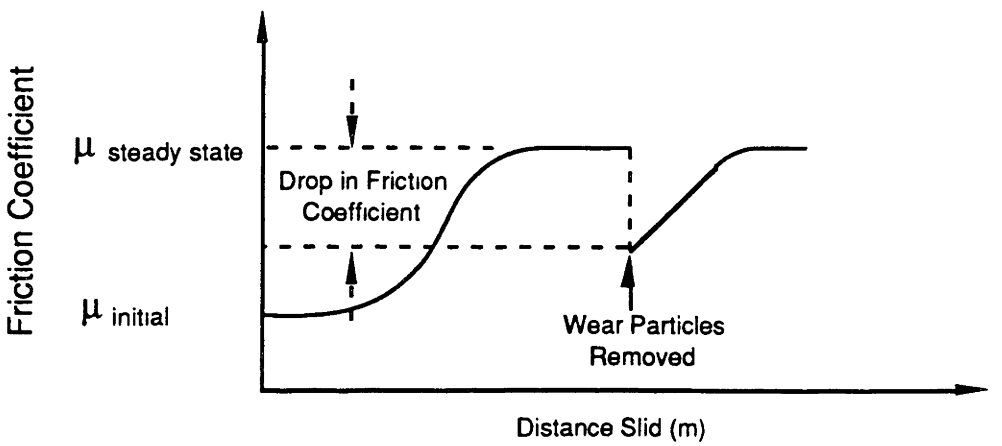


Figure 3: Friction Plot - Effects Due to Removal of Wear Particles

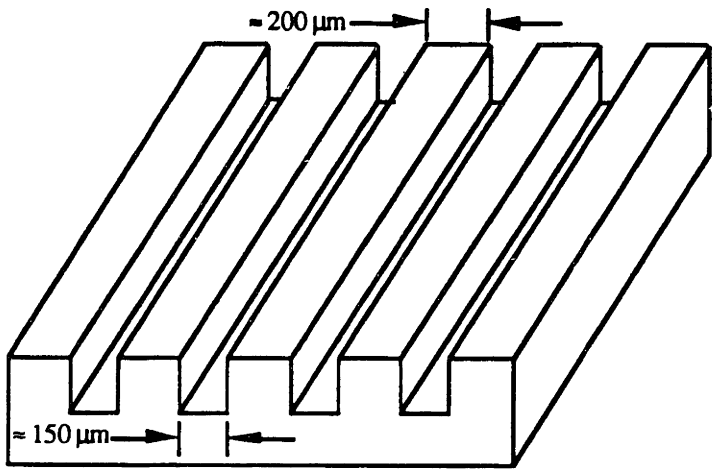


Figure 4: Typical Undulated Surface

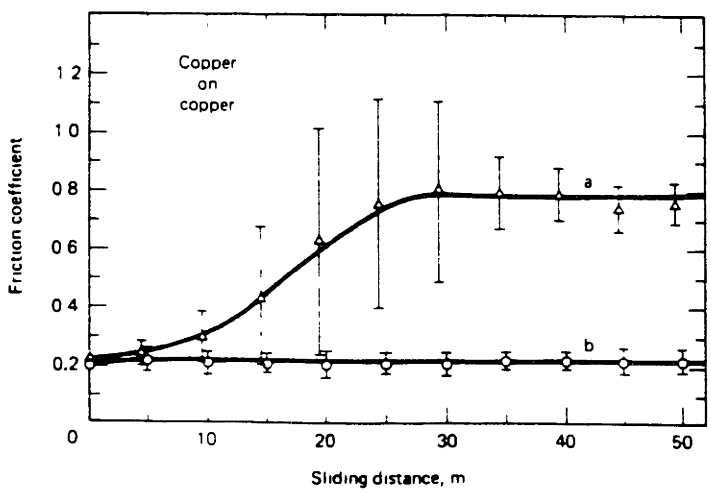


Figure 5: Friction Coefficient vs. Distance Slid: Copper on Copper, (a) Plain and (b) Undulated Surfaces [10]

The experiments on undulated surfaces clearly show that the adhesion effect is significantly lower than the mechanical effects. Furthermore, even at this level of low friction, it was observed that much of the friction was still due to mechanical interactions. Suh and Sin [9], and Komvopoulos *et al.* [12] also have shown that in theory, depending upon the sliding situation, friction coefficient values arising from asperity deformation can vary from 0.39 to 1, while adhesion can vary from 0 to 0.30 and plowing from 0 to 1.

## 1.2 Microscopic Investigations Into Friction

Since the invention of the Scanning Tunneling Microscope (STM) and the Atomic Force Microscope (AFM) [13-15] in the mid 1980s, atomic scale friction has been investigated by numerous authors [16-19]. Mate *et al.*, using AFM, have reported an extremely low dry sliding friction coefficient of 0.012 for 100 nm diameter tungsten stylus sliding on the basal plane of a single grain of polycrystalline graphite; the applied normal loads were in the range of $10^{-5}$ N. They have also reported the periodicity of the measured frictional force as atomic in nature (periodicity of the graphite surface atoms; see Figure 6). This implies that sliding had occurred elastically during the experiment. However, in contrast to these findings, Kaneko *et al.* [18], using STM, have reported a dry sliding friction coefficient of *infinity* for 20 μm diameter tungsten stylus sliding on a carbon sputtered surface; no normal load was used for this investigation. Although the experimental conditions of these two investigations were different, such large contrasts in the results make their interpretations difficult to decipher.

At a higher normal loads, friction experiments were conducted on Surface Force Apparatus, which was first used by Tabor and Winterton in 1969 [20-21]. This equipment enables the cleaved mica sheets, mounted on two half-cylindrical silica parts, to come into contact perpendicular to each other ("crossed cylinder configuration")

with separation distance controlled down to 0.1 nm. Under the normal loads of $10^{-2}$ to $10^{-1}$ N, the dry sliding friction coefficients of larger than one have been reported. However, with a thin film of $10^{-2}$ M KCl solution at the sliding interface, a low friction of 0.03 has been reported. The researchers claimed that even with a single monolayer of a film, sliding can occur without any surface destruction, i.e., elastic deformation at the contacting interface. One may suspect, however, that the interferometry technique (fringes of equal chromatic order) used by the researchers was not sensitive enough to detect the atomic scale surface damage. Furthermore, the high value of dry sliding friction coefficients was probably due to the low modulus of mica (extensive atomic scale surface and subsurface damage).

On the theoretical side, new insights into the modeling of the dynamic behavior of atoms, due to the availability of supercomputers, have enabled numerous researchers to study more readily the force interactions of discrete atoms (molecular dynamic simulation) [22-24]. The major shortcoming of these works is the questionable interface potential used to model the interaction at the interface. Another limitation is the limited number of atoms treated in the calculations; even $10^6$ atoms is not sufficient to incorporate all the necessary physics. Furthermore, the modeling of inherent material defects such as grain boundaries, impurities, and vacancies need to be developed further since the micro-mechanical behavior of solids are greatly affected by these defects. Therefore, such investigations still need further improvements before they can be considered reliable for any friction investigation.

Recently, Kim [25] has conducted friction experiments in *air* using hard and atomically smooth covalent and ionic solids under relatively low normal loads ($\approx 10^{-4}$ to $10^{-2}$ N). The measured friction coefficients varied from 0.06 to 0.13. His experiments have shown that plastic deformation *cannot* be prevented during contact sliding of crystalline solids under his experimental conditions. This

fact was evident from the pits observed upon chemical etching of the surfaces following the sliding test. It is believed that etch pits were the result of dislocations generated due to frictional interaction (see Figure 7). The experiments have also indicated that in air, microscopic frictional interactions are insensitive to material chemistry but are significantly influenced by the hardness and the roughness of the surfaces. However, it should be noted that the effects of material and surface chemistry may have been masked due to surface contamination and mild sliding conditions which may have hindered significant, if not all, generation of fresh surfaces.

## 1.3 Research Issues

The ultimate goal of the ongoing research is the creation and control of low friction surfaces through better understanding of the basic mechanisms of friction. The issue being raised in this thesis is: "what is the minimum friction when the mechanical effects are eliminated from the interface?" This question was raised as a direct result of previous investigations at M.I.T. during the past decade. They have shown, as stated previously, that contrary to past beliefs, mechanical interactions, rather than adhesion, are the dominant mechanisms of friction in most engineering situations. Therefore, by eliminating the mechanical interactions from the sliding interface, one can better understand interactions from the sliding interface, as well as be able to minimize and to gain better control over friction. More importantly, by understanding the fundamental mechanisms of friction, the mechanisms of wear can also be clarified since friction and wear are strongly related as described in the delamination theory of wear by Suh [26].

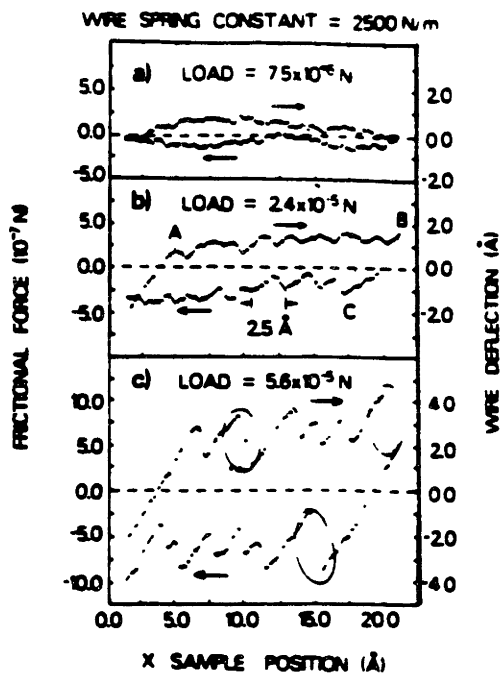


Figure 6: Results from Investigations by Mate *et al.* [17]

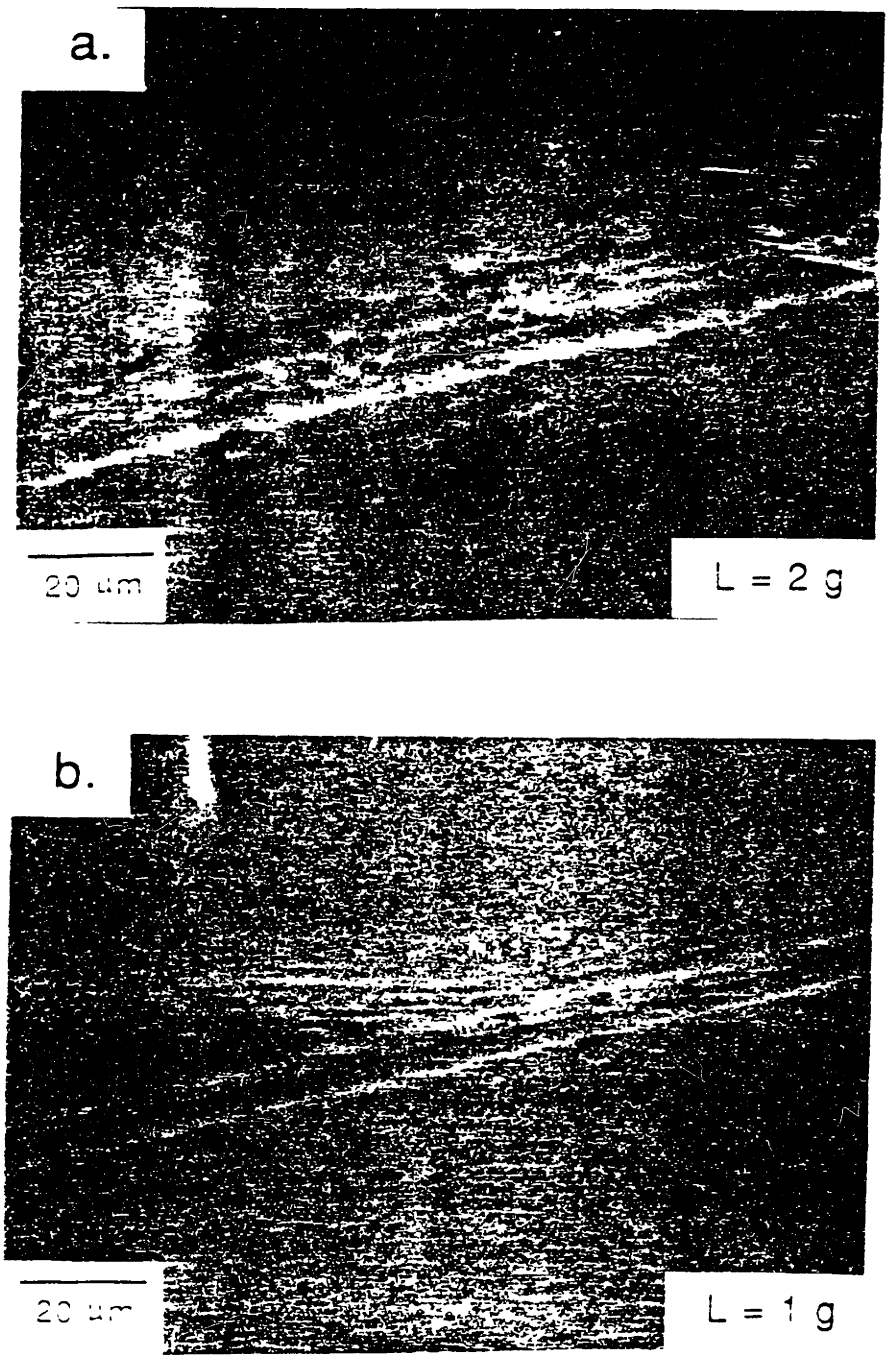


Figure 7: SEM Photograph of The Wear track of Si After Chemical Etching [25]

## 1.4 Impact of the Research

The success of this research on low friction and low wear will have a significant impact on both the science of tribology and on the technology for low energy consuming equipment and devices. Research will clarify present theories on the basic mechanisms of friction and provide a spring-board for further technological and scientific breakthroughs. The engineering implications of such ultra-low friction in dry sliding situations are limited only by the imagination. For example, the replacement of ball bearings with journal bearings of extremely low clearance will provide stiffness to the rotating devices, thus greatly improving the accuracy, reliability and durability of machines that use such bearings. Such advances should provide new technologies for the miniaturization of precision equipment. They can also be used in applications where lubrication is either cumbersome or impossible, including prosthesis, components to be used in space, and high temperature.

## 1.5 Outline of the Thesis

This thesis is divided into five chapters. Chapter 1 is the introduction. The past theories along with the most recent works on the inherent causes of friction will be discussed in this chapter.

Chapter 2 describes the different sets of friction experiments conducted in order to better understand the inherent causes of friction. Low loads and atomically smooth surfaces under many different test conditions were used. From these and other experiments conducted by Kim [25], it has been concluded that at present it is impossible to totally eliminate the mechanical interactions and that plastic deformation dominates friction phenomenon even in the absence of plowing by wear particles and very limited asperity interactions. In situations where mechanical interactions are totally eliminated, friction would be the result of atomic interactions involving van der Waals forces and formation of

chemical bonds. The insights gained from this research suggest that a sliding condition that involves only elastic interactions would lead to the minimum friction coefficient.

Chapter 3 describes the friction experiments conducted with elastomers made of natural rubber and sulfur. They were made for varying degrees of hardness in order to make the interface interactions elastic. Their hardness was varied to reach an optimum point in the mechanical behavior of the elastomer between the two extreme behaviors, i.e., viscoelastic and brittle behavior. This test provided guidance to the approach needed to reach the minimum friction in a dry-sliding situation. Finally, chapter 4 presents the conclusions of this thesis.

## 1.6 References


1. Bowden, F.P., and Tabor, D., The friction and Lubrication of Solids, Clarendon Press, Oxford, 1958, pp. 74-121.

2. Rabinowicz, E., Friction and Wear of Materials, John Weiley & Sons, 1965, pp. 37-38.

3. Moller, C.E., and Noland, M.C., "Cold Welding Tendencies and Frictional Studies of Clean Metals in Ultra-High Vacuum," *Trans. ASLE*, Vol. 10, 1967, pp. 146-157.

4. Buckley, D.H., "The influence of Crystal Structure, Orientation and Solubility on the Adhesion and Sliding of Various Metals and Single Crystals in Vacuum," Spec. Tech. Publ. 431, ASTM, 1967, pp 134-142.

5. Hehn, A.H. and Kimzey, J.H., "Adhesion of Metals and Nonmetals in Ultrahigh Vacuum," *J. Lub. Eng.*, June 1968, pp.274-285.

6. Bowden, F.P., and Childs, T.H., "The Friction and Deformation of a Clean Metals at Very Low Temperatures," *Proc. Roy. Soc.* A, Vol. 312, 1969, pp. 451-466.

7. Sargent, L.B., "On Fundamental Nature of Metal-Metal Adhesion," *Trans. ASLE*, Vol. 21, 1977, pp.345-370.

8. Buckley, D. H., "Definition and Effect of Chemical Properties of Surfaces in Friction, Wear, and Lubrication," in *Fundamentals of Tribology*, N.P. Suh and N. Saka, eds., MIT Press, Cambridge, MA., 1980, pp. 173-199.

9. Suh, N.P., and Sin, H.C., "The Genesis of Friction," *Wear*, Vol. 69, 1981, pp. 91-114.

10. Suh, N.P., Tribophysics, Prentice-Hall, New Jersey, 1986, pp. 88-89.

11. Tian, H.T., Saka, N., and Suh, N.P., "Boundary Lubrication Studies on Undulated Titanium Surfaces," *Tribology Transactions*, Vol. 32, No. 3, 1989, pp. 289-296.

12. Komvopoulos, K., Saka, N., and Suh, N.P., "Plowing Friction in Cry and Lubricated Metal Sliding," *J. of Tribology*, ASME Trans., Vol. 108, No. 3, July 1986, pp. 301-311.

13. Binnig, G., Quate, C.F., and Gerber, C., "The Scanning Tunneling Microscope," *Scientific American*, Vol. 253, No. 2, 1985, pp. 50-56.

14. Binnig, G., Quate, C.F., and Gerber, C., "Atomic Force Microscope," *Phy. Rev. Lett.*, Vol. 56, No.9, 1986, pp. 930-933.

15. Erlandsson, R., McClelland, G. M., Mate, C. M., Chiang, S., "Atomic Force Microscope Using Optical Interferometry", *J. Vac. Sci. Tech.*, Vol. A6, No. 2, 1988, pp. 266-270.

16. Skinner, N., Gane, N., and Tabor, D., "Micro-friction of Graphite," *Natural Physical Science*, Vol. 232, 1971, pp. 195-196.

17. Mate, C. M., McClelland, G. M., Erlandsson, R., and Chiang, S., "Atomic-Scale Friction of a Tungsten Tip on a Graphite Surface," *Phy. Rev. Lett.*, Vol. 59, No. 17, 1987, pp. 1942-1945.

18. Kaneko, R., Nonaka, K., and Yasuda, K., "Summary Abstract: Scanning Tunneling Microscopy and Atomic Force Microscopy of Microtribology," J. Vac. Sci. Tech., Vol. A6, No. 2, 1988, pp. 291-292.

19. Erlandsson, R., Hadziioannou, G., Mate, C. M., McClelland, G. M., and Chiang, S., "Atomic Scale Friction Between the Muscovite Mica Cleavage Plane and a Tungsten Tip," *J. Chem. Phy.*, Vol. 89, No. 8, 1988, pp. 5190-5193.

20. Tabor, D. and Winterton, R. H. S., "The Direct Measurement of Normal and Retarded van der Waals Forces," *Proc. Royal Soc. Lond.*, Vol. A312, 1969, pp.435-450.

21. Israelachvili, J. N. and Tabor, D., "The Measurement of van der Waals Dispersion Forces in the Range 1.5 to 130nm," *Proc. Royal Soc. Lond.*, Vol. A331, 1972, pp. 19-38.

22. Ribarsky, M. W. and Landman, U., "Dynamical simulations of stress, strain, and finite deformation", *Physical Rev. B*, Vol. 38, No. 14, 1988, pp. 9522-9537.

23. Belak, J. F. and Stowers, I. F., "A Molecular Dynamics Model of the Orthogonal Cutting Process," ASME Annual Meeting, Rochester, NY, 1990.

24. Belak, J. F. and Stowers, I. F., "Molecular Dynamics Studies of Surface Indentation in Two Dimensions," MRS Symposium: Atomic Scale Calculation of Structure in Materials, San Francisco, CA, 1990.

25. Kim, D., "Investigation of the Microscopic Mechanisms of Friction," Ph.D. Thesis, Dept. of M.E., M.I.T., May 1991, pp.95-126.

26. Suh, N.P., "The Delamination Theory of Wear," *Wear*, Vol. 25, 1973, pp. 111-124.

# Chapter 2

# Friction Experiments On Atomically Smooth Surfaces

## 2.1 Introduction

In the absence of mechanical effects, the sliding contact is elastic, and the frictional force is the resistance to sliding caused by the atomic attractions across the interface. Theoretically, an elastic sliding contact can be achieved when the stresses at the contacting asperities are maintained below the critical stress of the softer of the two sliding materials. In such a case, the atomic interactions can be controlled by proper selection of material composition and structure. Therefore, it is possible to choose a pair of sliding materials that has only van der Walls interatomic interactions such that the energy dissipation will be in the form of phonons generated as the surface atoms are perturbed from their equilibrium positions; the resulting frictional force will be extremely small. This statement is based on the premise that energy dissipated during plastic deformation is much greater in comparison with elastic deformation. Also, in elastic sliding, the wear is zero, thus providing a tremendous technological improvement. Furthermore, the apparent area of contact and the real area of contact can be made equal by applying a sufficient load; yet the stresses will be low enough so that the bulk deformation does not limit the contact area as in the plastic deformation situation. Therefore, frictional force can be controlled by simply reducing the area of contact.

In order to experimentally achieve an elastic (i.e., no viscoelastic or anelastic) sliding contact situation, the concept of low contact stress was utilized [1]; the minimization of mechanical interactions by reducing the contacting stresses at the asperities. In other words, the objective was to prevent plastic deformation of the contacting surfaces by using sufficiently low loads, but more

importantly, by assuring that the load is distributed over a large contact area. This concept can be algebraically explained by observing the Hertzian stress distribution of an asperity, modeled as a sphere, in contact with an ideally flat plate. The maximum stress, $\sigma_{max}$, for an elastic sphere of radius $\rho$ in contact with a semi-infinite flat plate under an applied normal load L is given by [1]:

$$\sigma_{max} = \left[ \frac{6L \left( \frac{1}{\frac{1-\nu_1^2}{E_1} + \frac{1-\nu_2^2}{E_2}} \right)}{\pi^3 \rho^2} \right]^{\frac{1}{3}} \qquad (2)$$

where E and $\nu$ are the Young's modulus and the Poisson's ratio, respectively. The subscripts 1 and 2 refer to the sphere and the plate respectively.

From the equation, one can state that the maximum stress is more effectively lowered by increasing $\rho$ rather than simply decreasing the applied normal load (L). The stresses at the contacts should be much lower with flat on flat configuration in comparison with the typical sphere on flat configuration. The limiting case of the low contact stress occurs when the real area of contact is equal to the apparent area of contact. At this point, the friction will be independent of the applied normal load and the friction coefficient can be minimized by simply decreasing the area of contact.

## 2.2 Apparatus

Since the conventional friction testing apparatus, such as pin-on-disk apparatus, are not appropriate for testing two flat specimens, a new friction apparatus was built and used for this

research (see Figures 8 and 9). Both the pin and the disk are physically constrained in the conventional apparatus, thus proper alignment of two flat surfaces would be a formidable task. The consequence of misalignment is the uneven distribution of the applied normal load, hence causing high stresses at a few localized regions. In the new apparatus, the proper alignment was achieved by utilizing gravity to simply rest a smaller sliding specimen over a larger stationary base specimen. The applied normal load was the weight of the sliding specimen itself.

The main component of the new apparatus was a hardened steel shim with dimensions 15.24 x 0.64 x 0.015 cm. One end of this shim was fixed to a rigid structure which was capable of fine vertical adjustment (0.0025 cm.). A 0.025 cm diameter and 1.91 cm long steel pin was attached to the free end of the beam. The sliding specimen, which was initially resting on a base specimen, was brought into a contact with this pin by the x-y table as shown in Figure 9. At this point, the overall component can be described as a beam fixed at one end and simply supported at the other end.

Since the weights of the sliding specimens were extremely small ($\approx 10^{-4}$ - $10^{-3}$ N), the method of applying a horizontal force to the sliding specimen had to be carefully thought out in consideration of a vibrational problem. A small vibration, induced by the method of applying a horizontal force (i.e., motor), could easily initiate the motion of the sliding specimen, thus creating misleading data. This problem was resolved by using a piezoceramic force actuating device, a cantilever beam structure with the beam being a piezoceramic bimorph. By applying DC voltage to the piezoceramic bimorph (beam), a horizontal displacement, corresponding to the applied voltage, was applied to the center of the beam, which in turn applied force to the sliding specimen (see Figure 9). The applied horizontal force was a ramp function, generated by an RC circuit as explained below and shown in Figure 10.

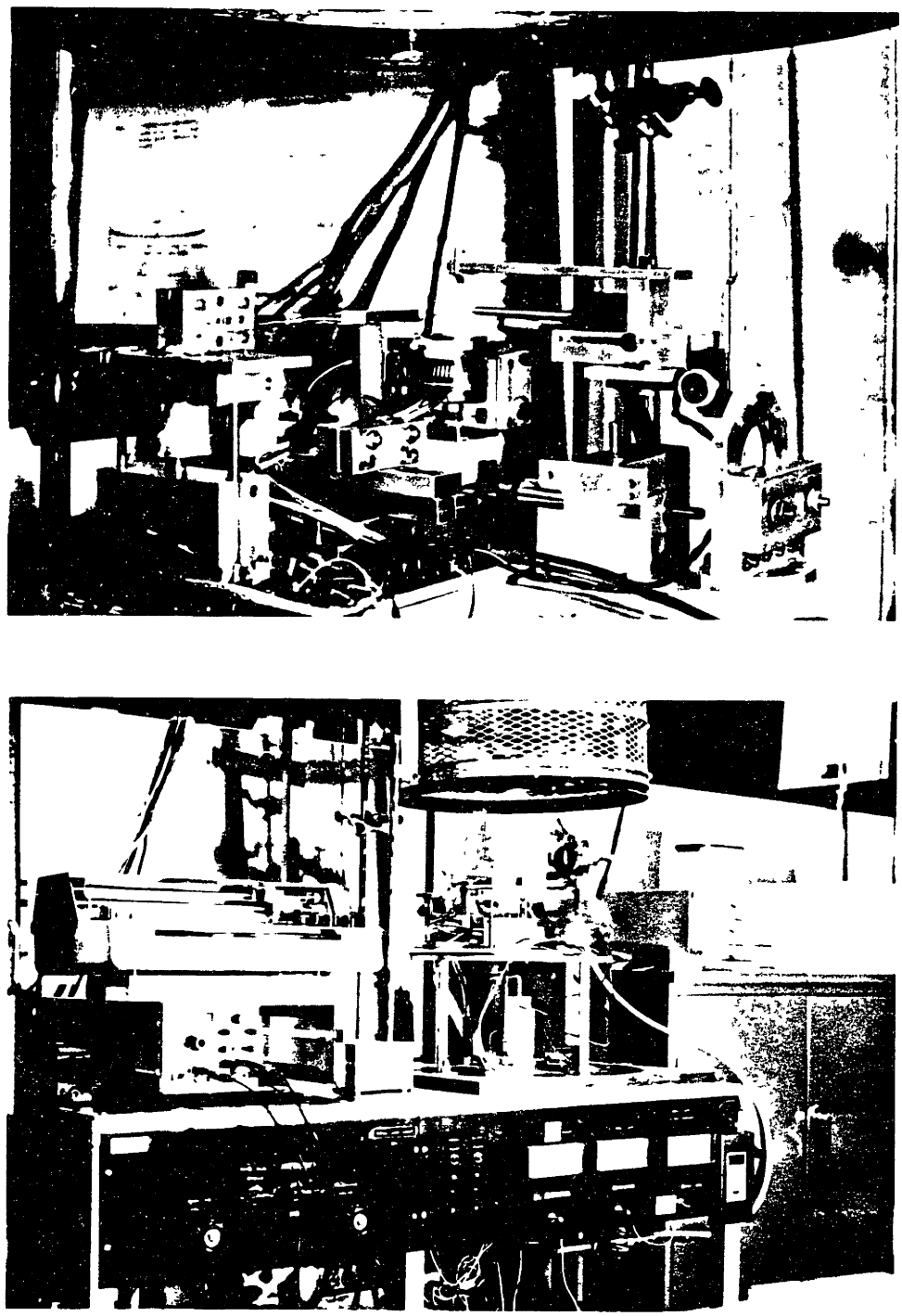

Figure 8: Piezoceramic - Friction Testing Apparatus - Photographs

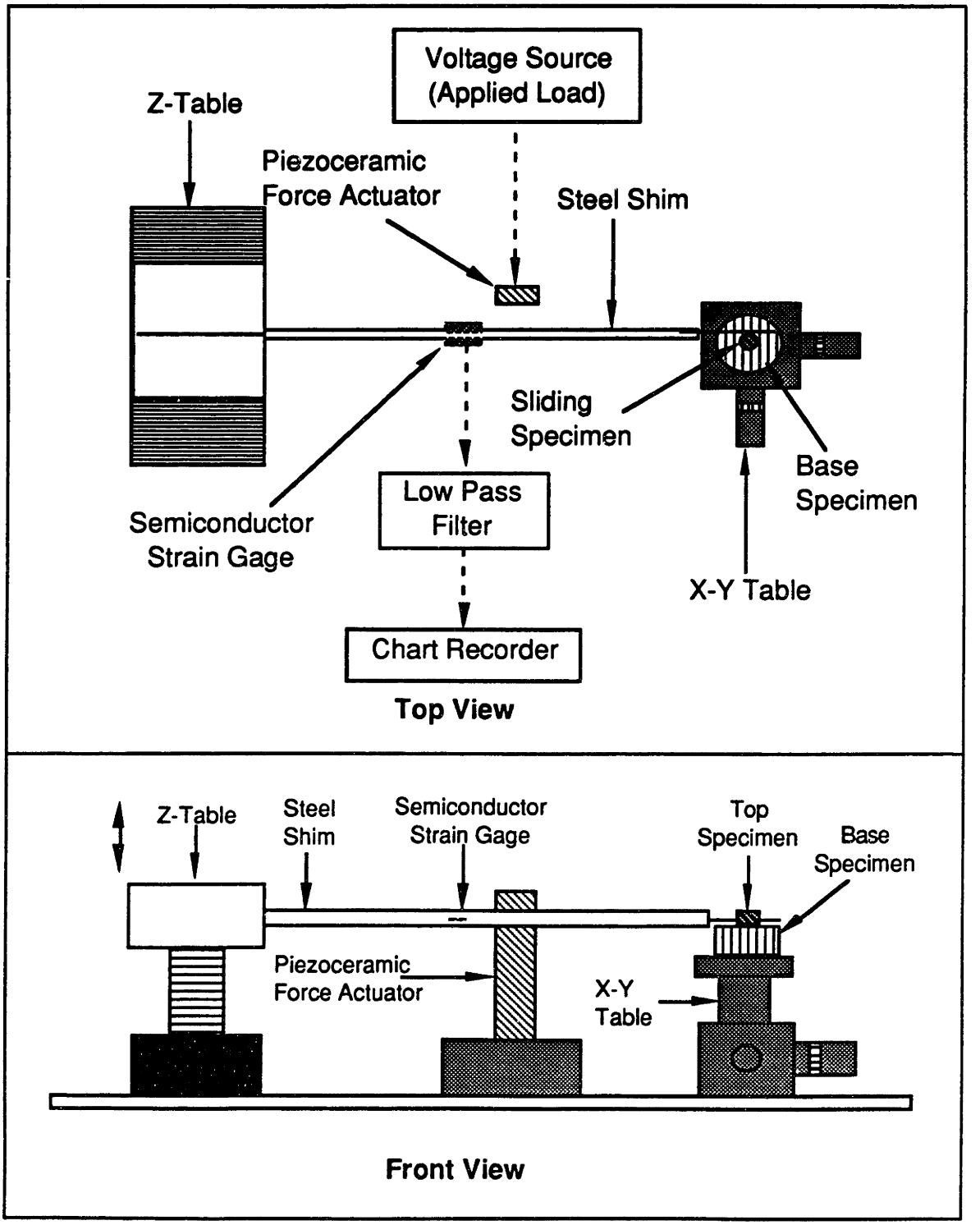


Figure 9: Piezoceramic - Friction Testing Apparatus - Schematic Drawing

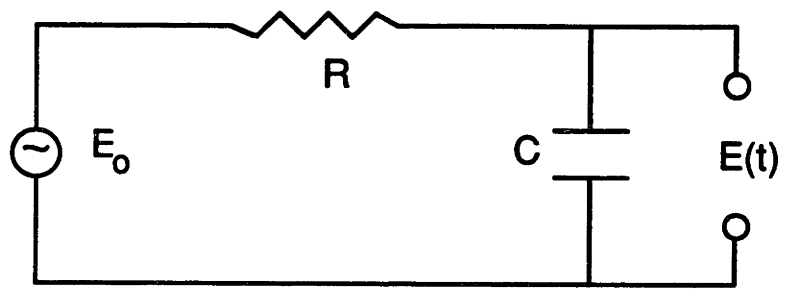


Figure 10: RC circuit: $E_o$ = Step Input; E(t) = Output

The RC circuit was a first order system that had an exponential response to a step input as described by the equation shown below and shown in Figure 11.

$$E(t) = E_o \left[ 1 - \exp(-t/RC) \right] \quad (3)$$

By an appropriate choice of R and C and by using the early portion of the time response ( $t < \tau$ ), it was possible to apply and control a ramp-like horizontal force to the sliding specimen at a very slow and steadily increasing rate of $1 \times 10^{-5}$ N / s.

The applied horizontal force was sensed by four semiconductor strain gages (gage factor of 155), which were attached to the steel beam and formed the four arms of the Wheatstone bridge. The output from the Wheatstone bridge had to first pass through the low pass filter and then to the chart recorder. The onset of sliding was detected as follows. When the horizontal force was applied to the beam, which was initially in contact with the sliding specimen, the beam underwent elastic bending and a straight line output response was recorded by the chart recorder as shown in Figure 12. Upon initiation of the slide, there was a distinct change in the slope of the output due to the change in the direction of beam bending. Therefore, it was possible to detect the exact moment of sliding with a resolution of approximately $1 \times 10^{-6}$ N.

Four air cushion isolators, "rubber donuts" were used in order to further ensure that the initial slippage was not due to vibration. For the experiments in air and in a clean room, the apparatus was enclosed in a rectangular box made of PMMA due to the shim's sensitivity to air currents.

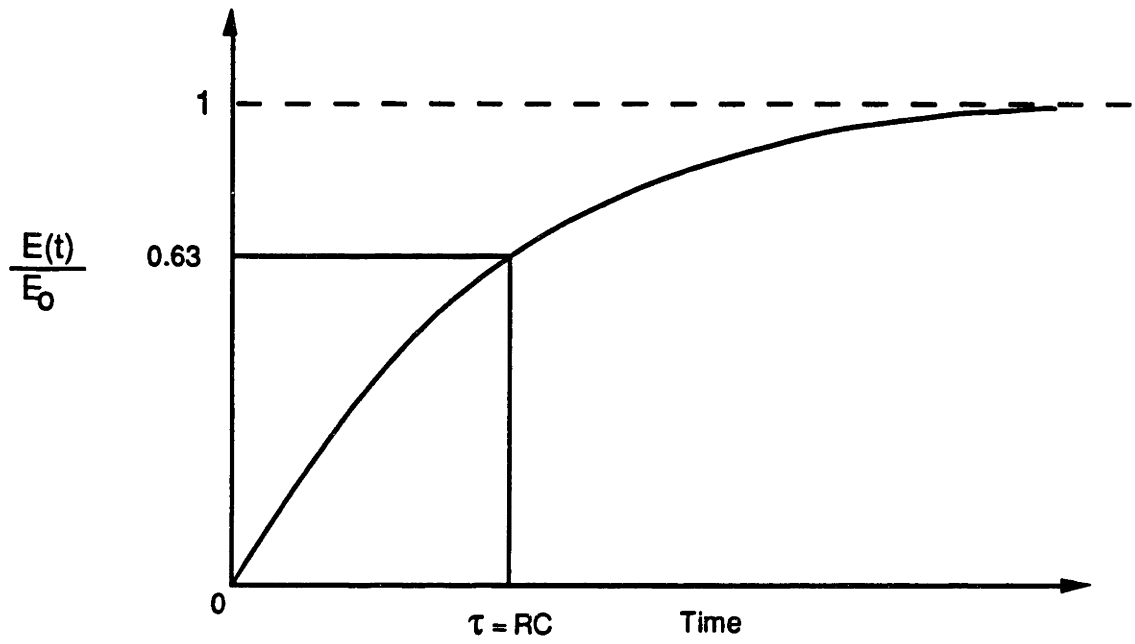


Figure 11: Response Plot of the RC Circuit

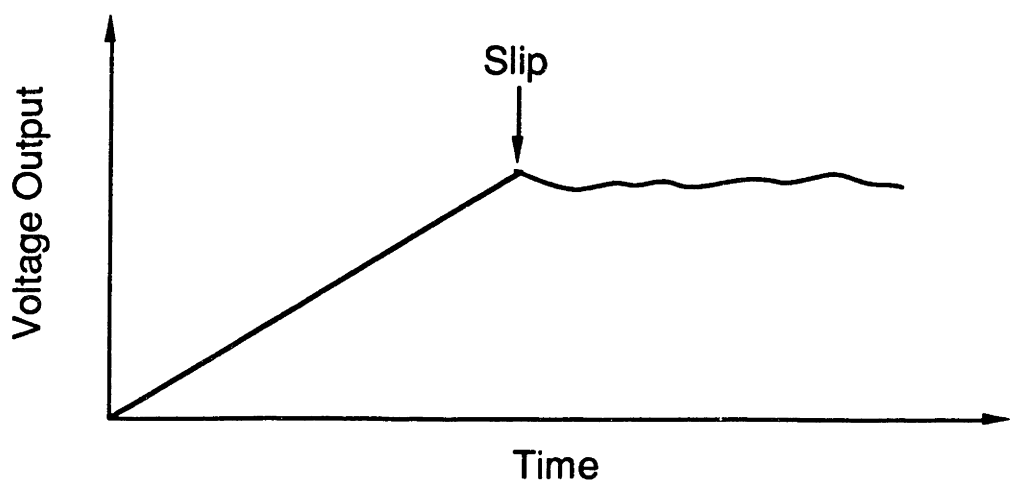


Figure 12: A Schematic Response from the Chart Recorder

## 2.3 Materials

Atomically smooth and hard samples were used for the experiments: silica glass [$SiO_2$], silicon wafer [Si (100)], and silicon carbide [SiC]. Pure silica glass was supplied by Photronic Corporation, N.Y. The glasses were highly polished in the middle as well as around the edge of the surface. Silica glass was the smoothest specimen available in the world (average roughness of 0.1 nm and the average flatness of approximately 30 nm). Silicon wafer was supplied by Aurel; a single crystal n-type silicon wafer, grown by Czochralski technique, was 0.3 mm thick with resistivity ranging from 4 to 6 $\Omega$ cm (average roughness of 1 nm and the average flatness of approximately 10 nm). Silicon carbide supplied by Lawrence Livermore National Laboratory, California, was the flattest specimen available in the world and under its own weight, the average contact pressure was only about 40 Pa (average roughness of 0.5 nm and the average flatness of approximately 5 nm). The average roughness and hardness of the samples are shown in Table 1. The optical profilometer (WYKO) printouts of the roughness and the flatness of the samples are shown in Figures 13 and 14.

## 2.4 Experiments in Ambient and in Clean Room

Using the piezoceramic friction testing apparatus, numerous tests were conducted with silica glass, silicon wafer, and silicon carbide as the base specimens and with silica glass and silicon wafer as the sliding specimens. The applied normal loads, or the weights, of the sliding specimens were (0.52 and 1.70) and (0.86 and 1.55) mN for silica glass and Silicon wafer respectively. The experimental conditions were as follows: (1) Ambient condition with temperature of approximately 25$^{o}$ C and humidity of around 30%; (2) Class 100 clean room with similar temperature and humidity in order to minimize the entrapment of dust particles at the sliding interface. For both types of tests, the specimens were ultrasonically cleaned in a bath of acetone as well as with an acetone soaked cotton tip. Large

portions of dust particles were blown away using a pressurized liquid form of chlorodifluoromethane, commercially known as "Dust-Off Plus", prior to testing.

### 2.4.1 Results from Ambient and Clean Room Experiments

The results from the experiments are shown in Tables 2 and 3. The experimental results show that the friction coefficients were low and were approximately 0.1 for all combinations and conditions with the values ranging from 0.08 to 0.13. For all combinations, the results were repeatable, thus friction coefficients had very small standard deviations (0.01 - 0.04). All combinations where silicon carbide (flattest specimen) was used as a base specimen had the lowest mean friction coefficients and standard deviations. This seems to suggest that the combinations involving silicon carbide had the lowest asperity contact stress (applied normal load was distributed the most with respect to other combinations) and as a consequence, must have had a larger portion of the real area of contact undergoing elastic deformation in comparison to other combinations (see section 2.4.2 for details). In contrast, all combinations involving silica glass, the smoothest yet least flat specimen, had the highest mean friction coefficients and standard deviations. It should also be noted that the frictional forces were directly proportional to the applied normal loads in the range used in the experiments. Finally, for all cases, the surface damage could not be detected by an optical microscope, scanning electron microscope, environmental scanning electron microscope (no gold coating required for observation of the surface of specimens), Dektek surface profilometer, or even after the surfaces were chemically etched.

Table 1: Average Roughness and Hardness of the Specimens

| Specimens | Average Roughness (nm) | Hardness (MPa) |
|---|---|---|
| Silica Glass ($SiO_2$) Disk & Slider | 0.1 | 6500 |
| Silicon Wafer (Si) Disk & Slider | 1.0 | 8200 |
| Silicon Carbide (SiC) Disk | 0.5 | 34000 |

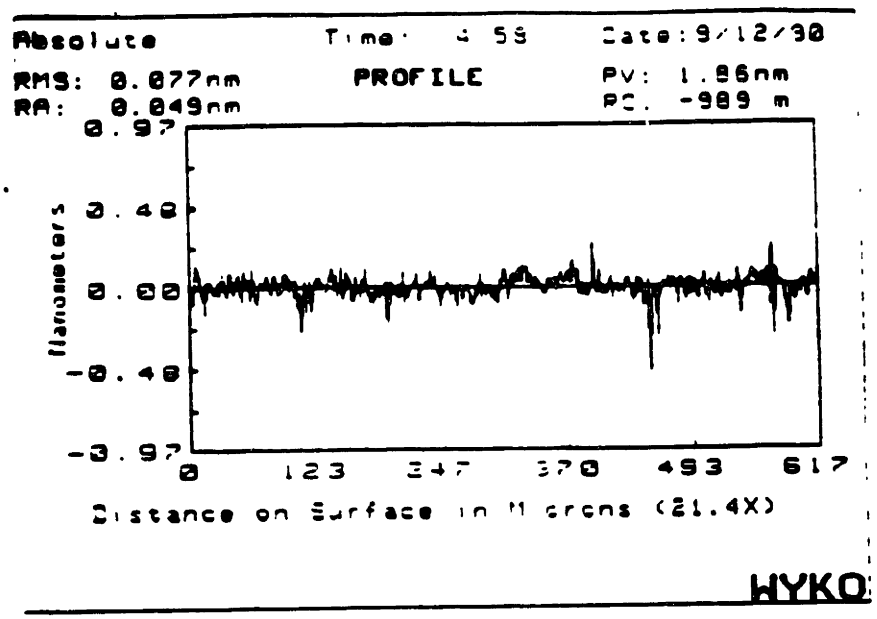


(a)

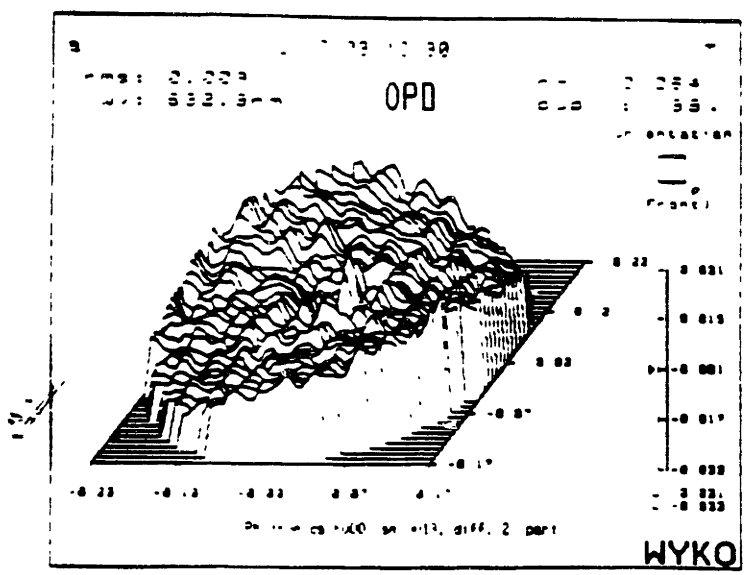


(b)

Figure 13: Optical Profilometer Printouts of $SiO_2$: (a) Roughness (b) Flatness

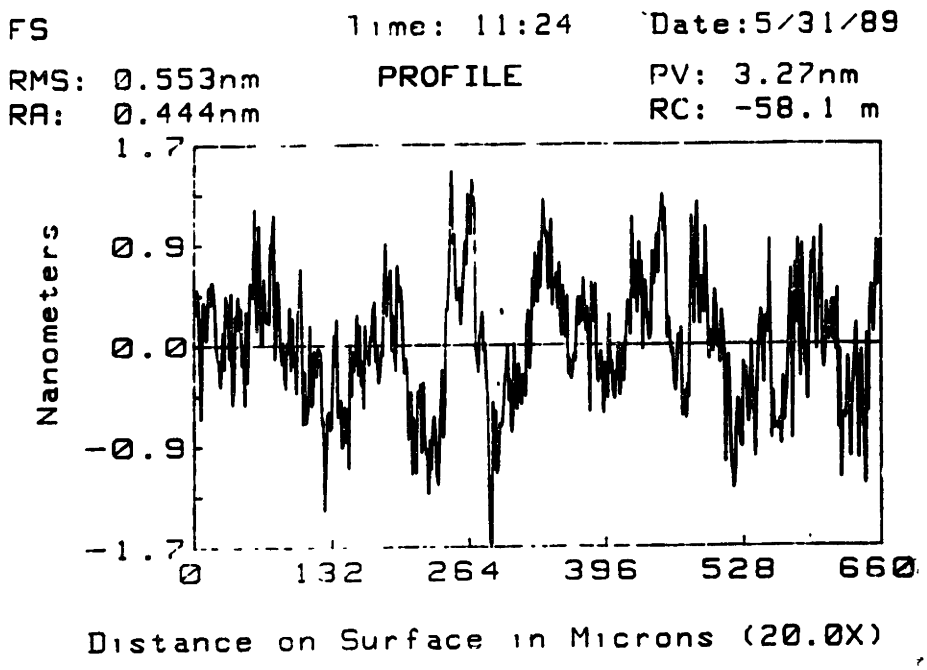


(a)

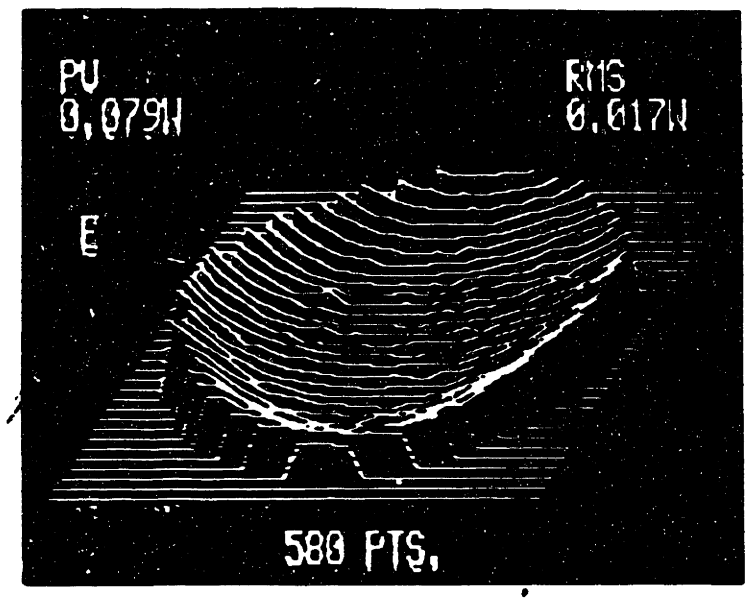


(b)

Figure 14: Optical Profilometer Printouts of SiC: (a) Roughness (b) Flatness

Table 2: Friction Coefficients from Ambient Experiment

| Slider | Base | Load (mN) | Mean Friction Coefficient | Standard Deviation |
|---|---|---|---|---|
| Silica Glass | Silica Glass | 0.52 | 0.13 | 0.04 |
| Silica Glass | Silicon Wafer | 0.52 | 0.12 | 0.02 |
| Silica Glass | Silicon Carbide | 0.52 | 0.10 | 0.02 |
| Silica Glass | Silica Glass | 1.70 | 0.13 | 0.03 |
| Silica Glass | Silicon Wafer | 1.70 | 0.12 | 0.03 |
| Silica Glass | Silicon Carbide | 1.70 | 0.11 | 0.02 |
| Silicon Wafer | Silica Glass | 0.86 | 0.13 | 0.02 |
| Silicon Wafer | Silicon Wafer | 0.86 | 0.10 | 0.02 |
| Silicon Wafer | Silicon Carbide | 0.86 | 0.10 | 0.01 |
| Silicon Wafer | Silica Glass | 1.55 | 0.12 | 0.03 |
| Silicon Wafer | Silicon Wafer | 1.55 | 0.11 | 0.03 |
| Silicon Wafer | Silicon Carbide | 1.55 | 0.09 | 0.02 |

Table 3: Friction Coefficients from Clean Room Experiment

| Slider | Base | Load (mN) | Mean Friction Coefficient | Standard Deviation |
|---|---|---|---|---|
| Silica Glass | Silica Glass | 0.52 | 0.12 | 0.04 |
| Silica Glass | Silicon Wafer | 0.52 | 0.12 | 0.02 |
| Silica Glass | Silicon Carbide | 0.52 | 0.10 | 0.02 |
| Silica Glass | Silica Glass | 1.70 | 0.13 | 0.03 |
| Silica Glass | Silicon Wafer | 1.70 | 0.12 | 0.02 |
| Silica Glass | Silicon Carbide | 1.70 | 0.09 | 0.02 |
| Silicon Wafer | Silica Glass | 0.86 | 0.13 | 0.03 |
| Silicon Wafer | Silicon Wafer | 0.86 | 0.11 | 0.02 |
| Silicon Wafer | Silicon Carbide | 0.86 | 0.09 | 0.01 |
| Silicon Wafer | Silica Glass | 1.55 | 0.12 | 0.03 |
| Silicon Wafer | Silicon Wafer | 1.55 | 0.11 | 0.03 |
| Silicon Wafer | Silicon Carbide | 1.55 | 0.08 | 0.02 |

### 2.4.2 Conclusions from Ambient and Clean Room Experiments

The fact that surface damage is undetectable does not necessarily imply that the sliding has occurred elastically and that the resulting frictional forces were due to interatomic interactions at the sliding interface. Rather, there is reason to suspect that the sliding did indeed involve plastic deformation but that this deformation was too small to be detected by the techniques used. The reason for this suspicion is that the resulting friction coefficients were virtually equal to the friction coefficients obtained at higher applied normal loads, where surface damage was clearly exposed by the chemical etching technique [1]. Therefore, it is reasonable to state that similar mechanisms of friction must have contributed to the frictional force for the lower load experiment as well.

Another argument in favor of plastic deformation is given as follows [1]: If the asperity contact involves plastic deformation, it is reasonable to assume that the sliding contact must also involve plastic deformation. Furthermore, one can readily infer that sliding contact has occurred plastically, simply by observing the relationship between the frictional force and the applied normal load. The explanation for this statement is as follows: The asperities are modeled as spheres that are in elastic contact with a semi-infinite flat plate. The model then presents the following two possibilities: (1) As the load increases, the number of asperities in contact with the plate remains the same, but the radius of each contact increases. In this case, the real area of contact will vary to the power of 2/3 of the applied normal load, and since the frictional force is directly proportional to the real area of contact, the frictional force itself should also vary to the 2/3 power, as shown below:

$$F \propto L^{2/3} \tag{4}$$

(2) As the load increases, the number of asperities in contact increases, but the radius of contact remains the same. In this case, the frictional force is directly proportional to the applied normal load.

$$F \propto L^{1} \tag{5}$$

In reality, a combination of both possibilities may arise for a given sliding condition. Therefore, the frictional force can vary anywhere between a two-thirds and a first power of the applied normal load for the elastic sliding condition. Table 4 summarizes the above ideas and shows how much the frictional force will increase as the applied normal load is increased.

It is well known that if a sliding contact involves plastic deformation, then the frictional force is directly proportional to the applied normal load. Upon comparing Table 4 and the experimental results, it is clear that plastic deformation must have occurred during the sliding experiments, i.e., the frictional forces were directly proportional to the applied normal load.

Although it is possible to argue that plastic deformation must have occurred during the experiments, it remains unclear whether this form of deformation was the major contributor to the total frictional force ($\mu \approx 0.1$). Even on an atomic scale, the geometrical constraints should allow some elastic deformation, which involves forming and breaking of atomic bonds at the sliding interface, to occur (see Figure 15). Therefore, it may be incorrect to extrapolate from the conclusions of macroscopic or high friction regimes (where adhesion effect is much less than the mechanical effect) and thus conclude that the contribution by the nonmechanical effects was small or even negligible in this experiment as well. The extent of the

contribution by interatomic interactions (i.e., elastic deformation, adhesion) still needs to be clarified.

If one assumes that the effects due to adhesion are insignificant (which will be proven in the next set of experiments), then the fact that all combinations involving silicon carbide resulted in the lowest mean friction coefficients can be explained as follows: The tests involving silicon carbide (flattest specimen) had the lowest asperity contact stress (the applied load was distributed more than other test combinations) and as a consequence, must have had a larger portion of the real area of contact undergoing elastic deformation (in comparison to other test combinations). The remaining portion of the real area of contact, which underwent plastic deformation, must have been smaller. Therefore, less energy was dissipated in the form of dislocation generation and motion. Furthermore, the fact that silicon carbide was the hardest specimen may also have contributed to less plastic deformation and plowing by submicron particles. Therefore, the overall energy dissipation or the friction was smallest when the silicon carbide was used as a base specimen.

In the next series of experiments, the endeavor was to understand the effects on the friction due to surface contamination by adsorption (i.e., water molecules, inert gas molecules, etc.). The hypothesis was that adhesion effects would be substantially improved by removing most of the adsorbed molecules from the surfaces. If adhesion effect is of any significance, an increase in adhesion should result in an increase in friction coefficients although the effects due to plastic deformation will remain virtually the same. Therefore, it was decided that similar experiments (i.e., clean room condition) needed to be conducted in a high vacuum with heated surfaces.

Table 4: Theoretically Predicted Value of an Increase in the Frictional Force - Elastic Contacts

| Normal Load Increased by a Factor of | Increase in the Frictional Force for 2/3 Power | Increase in the Frictional Force for 1 Power |
|---|---|---|
| 2 | 1.6 | 2 |
| 3 | 2.1 | 3 |
| 4 | 2.5 | 4 |

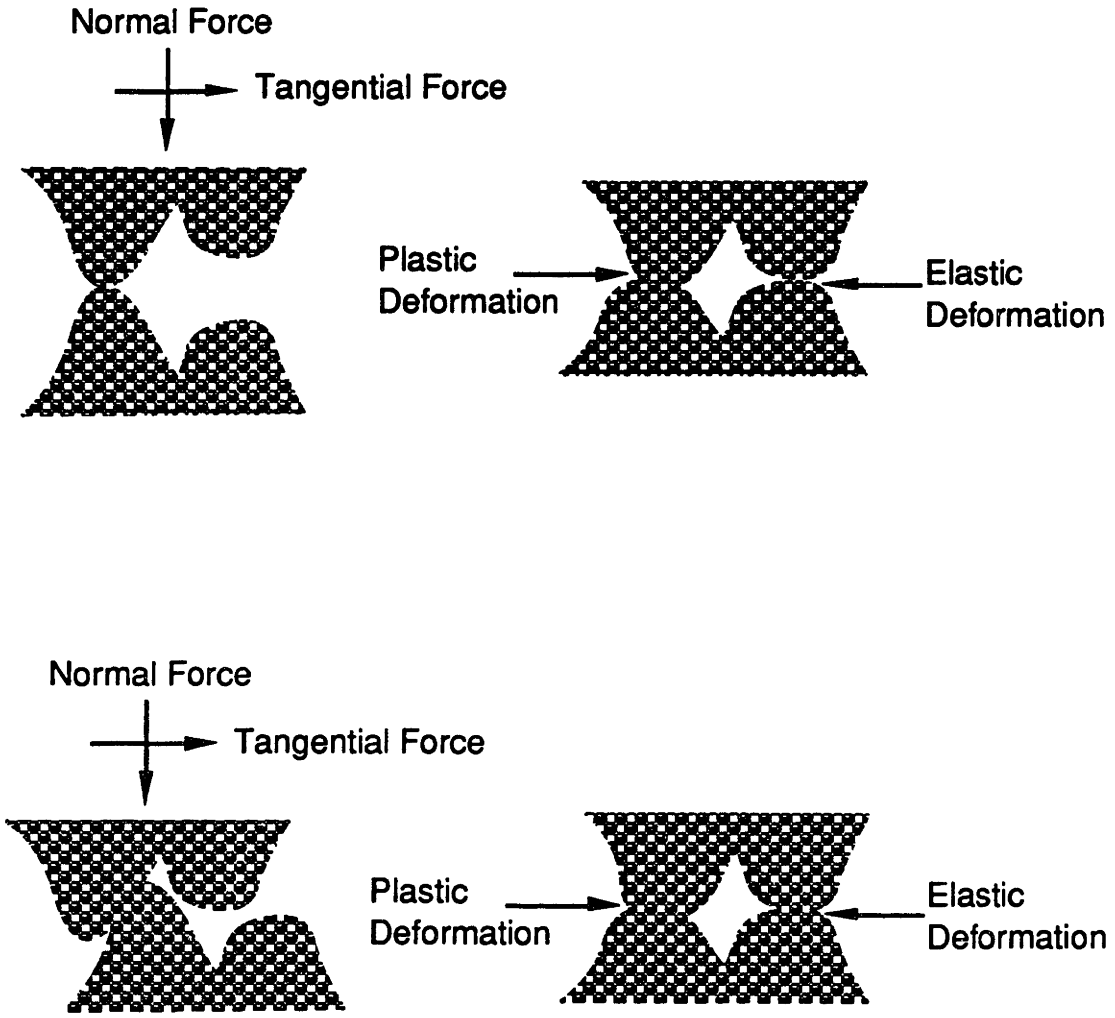


Figure 15: Surface Contact Possibilities

## 2.5 Experiments in Vacuum

### 2.5.1 Preparation for the Experiment

The surface of the specimen was heated up to 400° C inside a vacuum chamber ($1x10^{-5}$ Torr) in order to eliminate the water molecules and adsorbed gases from the sliding interface. This condition corresponds to the removal of both physically and chemically adsorbed molecules from the surface of the glass (see Appendix A and section 2.5.3 for details). The piezoceramic friction tester was modified to work inside a vacuum chamber (see Figure 16).

One major new component (the solenoid holder) needs to be explained. This device was built in order to initially separate the sliding specimen from the base specimen and then to be able to bring the two surfaces into contact once the desired pressure and the temperature was reached. This was accomplished by first having the sliding specimen compressed between a shaft and a "fixed end" by a spring (see Figure 17). Then, the shaft was pulled back by applying a voltage to the solenoid, upon which the sliding specimen was released and rested on the base specimen.

### 2.5.2 Experimental Procedure

The experimental procedure was as follows: The specimens were cleaned ultrasonically in a bath of acetone. They were then separated (1 mm apart) using the "solenoid holder" and heated to 400° C. While the specimens were being heated, the vacuum chamber was pumped down to 30 milliTorr by the mechanical pump. A stream of clean, filtered, and dry nitrogen gas was allowed to strike the surface of the specimens in order to remove the dust particles that settled onto the surfaces during evacuation. Even in a vacuum, large dust particles do not necessarily get "pumped out". The vacuum chamber was then pumped down to $10^{-5}$ Torr by the diffusion pump. Then the samples were brought into contact and

were left for few minutes. The procedure then continued exactly as in the air condition. Silica glasses, weighing 0.52 and 1.70 mN were used as the sliding specimens. Silica glass, Si, and SiC were the base specimens.

Another, type of experiment was also conducted; this time to observe the behavior of friction as a function of surface temperature (25 - 400° C) as well as to insure that the results at 400° C was not at the beginning, middle, and end of a certain trend. For this experiment, 1.70 mN silica glass was used as the slider while silica glass and SiC were the base specimens.

### 2.5.3 Results from the Vacuum Experiments

The results of the experiments are shown in Tables 5 and 6 and in Figures 18 and 19. The experimental results showed that the friction coefficients were once again low and were approximately 0.1 for all combinations and conditions with values ranging from 0.09 to 0.13. For all combinations, the results were very repeatable, thus friction coefficients had very small standard deviations (0.01 - 0.04). Neither vacuum nor vacuum+heat had any effect; the effects of adsorbed molecules seem very minimal at best. All combinations where silicon carbide (flattest specimen) was used as a base specimen had the lowest mean friction coefficients and standard deviations. In contrast, all combinations involving silica glass, the smoothest yet least flat specimen, had the highest mean friction coefficients and standard deviations. Also, the resulting friction coefficients remained constant between 25 and 400° C. This shows that the results at 400° C were not at the beginning, middle, and end of a certain trend. All of these observations suggest that the same mechanisms of friction must have occurred in air and in vacuum+heat. Once again, the surface damages could not be detected. However, the resulting frictional forces were also once again directly proportional to the applied normal load, suggesting that the plastic deformation had been present.

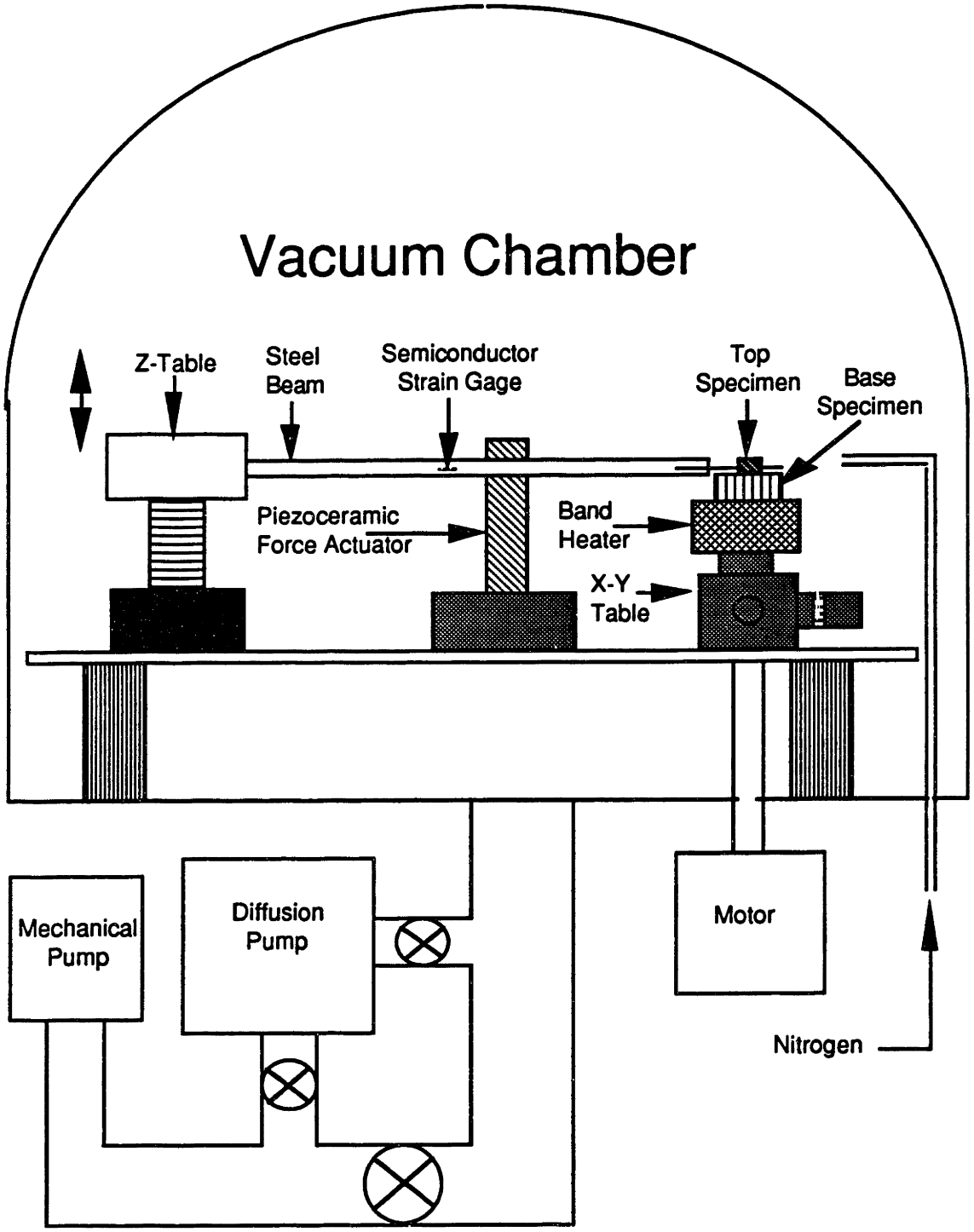


Figure 16: Piezoceramic Friction Testing Apparatus - modified

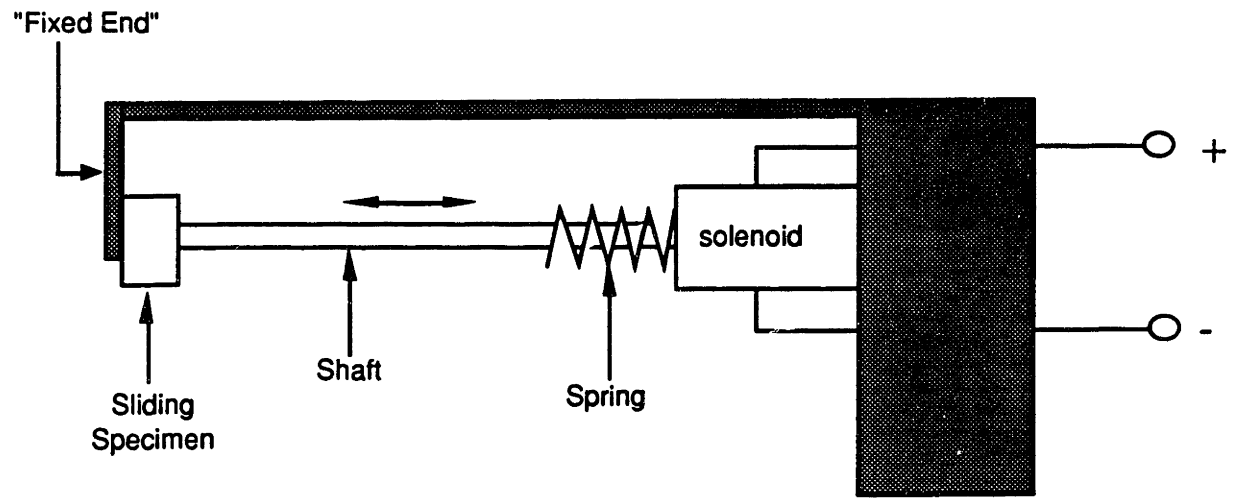


Figure 17: The "Solenoid Holder"

Table 5: Friction Coefficients from Vacuum (25° C) Experiment

| Slider | Base | Load (mN) | Mean Friction Coefficient | Standard Deviation |
|---|---|---|---|---|
| Silica Glass | Silica Glass | 0.52 | 0.13 | 0.04 |
| Silica Glass | Silicon Wafer | 0.52 | 0.12 | 0.02 |
| Silica Glass | Silicon Carbide | 0.52 | 0.09 | 0.03 |
| Silica Glass | Silica Glass | 1.70 | 0.13 | 0.03 |
| Silica Glass | Silicon Wafer | 1.70 | 0.12 | 0.02 |
| Silica Glass | Silicon Carbide | 1.70 | 0.10 | 0.02 |

Table 6: Friction Coefficients from Vacuum + Heat (400° C) Experiment

| Slider | Base | Load (mN) | Mean Friction Coefficient | Standard Deviation |
|---|---|---|---|---|
| Silica Glass | Silica Glass | 0.52 | 0.13 | 0.03 |
| Silica Glass | Silicon Wafer | 0.52 | 0.11 | 0.02 |
| Silica Glass | Silicon Carbide | 0.52 | 0.10 | 0.02 |
| Silica Glass | Silica Glass | 1.70 | 0.12 | 0.04 |
| Silica Glass | Silicon Wafer | 1.70 | 0.11 | 0.02 |
| Silica Glass | Silicon Carbide | 1.70 | 0.10 | 0.01 |

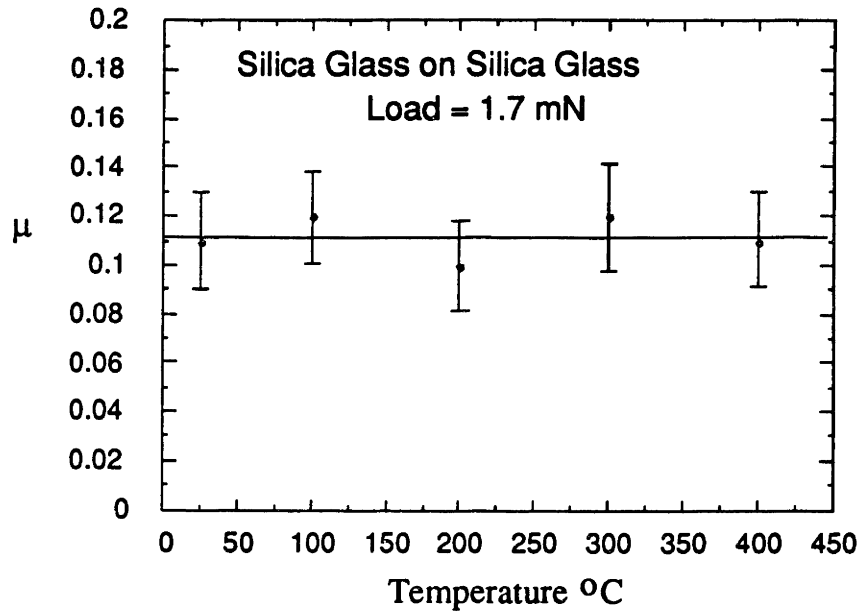


Figure 18: Static Friction Coefficient vs. Temperature: Slider - Silica Glass, Base - Silica Glass

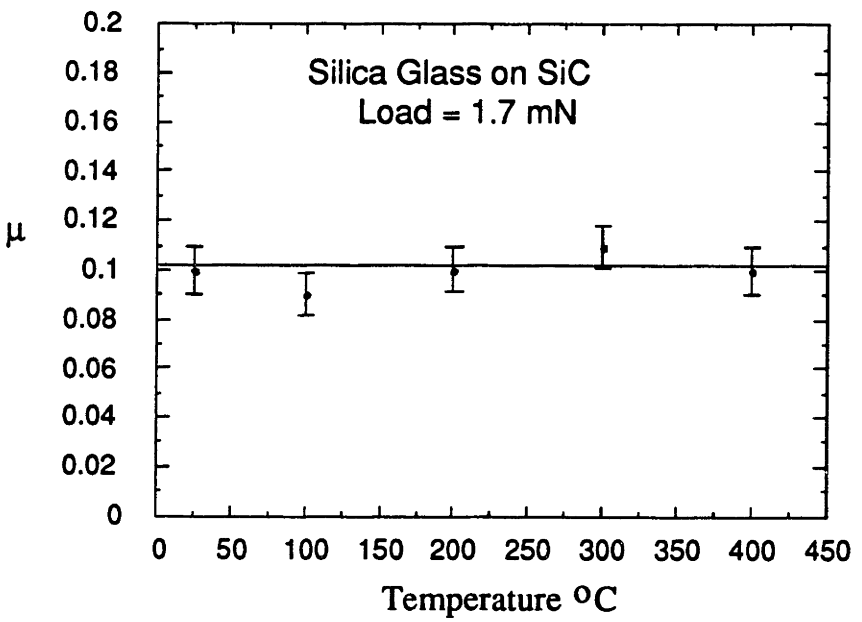


Figure 19: Static Friction Coefficient vs. Temperature: Slider - Silica Glass, Base - SiC

### 2.5.4 Discussion and Conclusions from Vacuum Experiments

#### 2.5.4.A Surface of Glasses

The principal gases found on the surface of most glasses are water vapor, carbon dioxide, sulfur dioxide, and oxygen. The water molecules are usually the most abundant and are held to a glass surface by either chemical or physical forces, whereas inert gas molecules are only physically bound and the glass temperature must be greatly reduced for measurable adsorption to occur.

According to Sherwood [2] and Harris and Schumacher [3] the maximum desorption of the gases from the surface of the glass occurs at 200 - 400° C for most glasses (see Figure 20). They also claim that the rapid rise in the desorption around 500° C is due to large quantities of "water" vapor being released as a result of the thermal decomposition of the glass itself (migration of OH ion from the interior). It should be noted that the exact temperature of desorption maximum does not depend solely on the nature of the glass, rather it depends on the combined effects of the nature of glass and the thermal cycle used in the specific experiment [4].

Large quantities of gas does not seem to adsorb on silica glass ($SiO_2$). Thus Garbe and Christians [4] degassed a silica flask at about 1000° C in vacuum and then exposed it to air. The flask was then repumped to $10^{-7}$ Torr and baked; liberating 3.7 x $10^{-5}$ $cm^3$ N.T.P./$cm^2$ of gas at 380° C rising to 6.1 x $10^{-5}$ $cm^3$ N.T.P./$cm^2$ of gas at 480° C. The important point is that these quantities were consistent with the desorption of a *chemisorbed* monolayer.

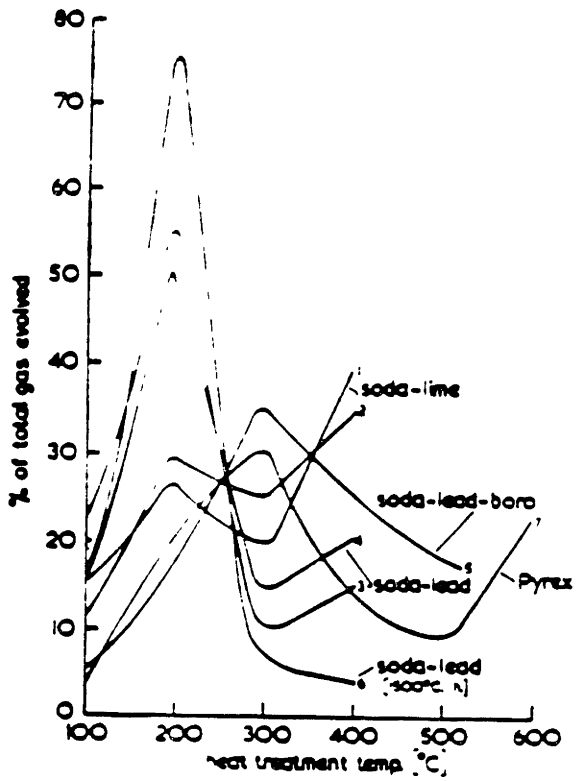


Figure 20: Desorption from Glass Surfaces [4]

### 2.5.4.B Surface Conditions of Si and SiC

The formation of the oxide layer on the surface of Si can be viewed as a multi-step process: (1) The oxide layer begins with the initiation of the first monolayer of oxygen; the oxygen molecules must adsorb onto the surface by dissociative adsorption:

$$O_2\,(g) \longrightarrow 2\,O\,(ad)$$

or, by adsorbing as a molecule and then dissociating on the surface:

$$O_2\,(g) \longrightarrow O_2\,(ad)$$
$$O_2\,(ad) \longrightarrow 2\,O\,(ad)$$

(2) The adsorbed oxygen atoms then combines with Si (surface atoms) to form silicon monoxide (SiO), which is volatile at temperatures above 1073° K.

$$Si\,(s) + O\,(ad) \xrightarrow{T > 1073^{o}\,K} SiO\,(g)$$

$$Si\,(s) + O\,(ad) \xrightarrow{T < 1073^{o}\,K} SiO\,(ad)$$

(3) The final step in the formation of the oxide layer is the bonding of another oxygen atom to the monoxide to form silicon dioxide.

$$SiO\,(ad) + O\,(ad) \longrightarrow SiO_2\,(ad)$$

Since $SiO_2$ is stable at temperatures below its melting point (1400° C), once the "first layer" of $SiO_2$ forms, the further growth of $SiO_2$ becomes "passivated," or rate limited by the diffusion of oxygen atoms through the oxide layer to the bulk [5]. Therefore, the adsorption of gas molecules on the surface of Si should be very similar to those of silica glass. Yabumoto *et al.* [6], like Garbe and Christian, found that the maximum desorption of Si occurred around 300 to 450° C as shown in figure 21.

The previous work [7] has also indicated that after bakeout in an ultra-high vacuum, a carefully prepared and handled SiC sample exhibited one to two monolayers of $SiO_2$. The surface oxide bonds only to the Si, as confirmed by the observation of Auger electron spectroscopy (AES) line shapes. Although the surface of the SiC is not completely covered with $SiO_2$, it is reasonable to assume that the adsorption of gas molecules on the surface of the SiC should be at least similar to that of silica glass since the $SiO_2$ portion of the surface will still behave like silica glass.

### 2.5.4.C Conclusions

From the literature, the optimal temperature for the desorption seemed to be around 300-400° C for all three specimens since higher temperatures may lead to thermal decomposition of the glass itself. Furthermore, a low pressure of $1x10^{-5}$ Torr was also used to prevent readsorption of desorbed molecules (see Appendix I for details). Therefore, the experimental conditions should have greatly minimized the physically and chemically adsorbed molecules (i.e., water, carbon dioxide, etc.) on the surface of the specimens and thus led to highly favorable conditions required for strong adhesion at the sliding interface.

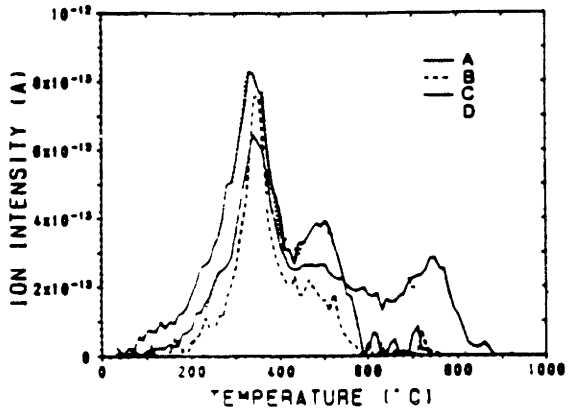


Desorption Spectra of Water

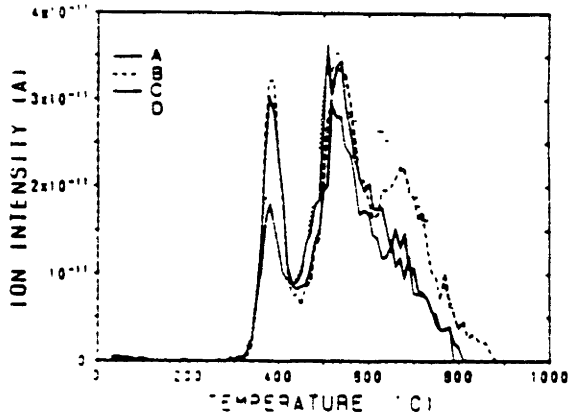


Desorption Spectra of $H_2$

Figure 21 Desorption from Si Surface: [6]

The experiments in vacuum and vacuum+heat indicate that for crystalline solids, both macro- and micro-frictional behavior is dominated by mechanical interactions at and below the sliding interface. The adhesion, which occurred at elastically deformed asperity junctions, seemed to be an insignificant contributor to friction. This can be concluded from two observations. First, similar values of friction coefficients ($\approx$ 0.1) were obtained for dry sliding of various atomically smooth, hard, and flat surfaces under low loads ($10^{-1}$ to $10^{-2}$ N, surface and subsurface damage detected by chemical etching of the surfaces) and extremely low loads ($10^{-3}$ to $10^{-4}$ N, non-detectable surface damage). This suggests that the same mechanisms of friction must have occurred in both situations. Furthermore, as shown in section 2.4.2, the direct proportionality between the the applied normal load and the resulting frictional force also suggests that plastic deformation must have occurred during sliding. Even atomic scale roughness (0.1 nm) was large enough to cause mechanical interactions in the form of dislocation generation and motion.

Second, adsorbed molecules had negligible effects on friction; vacuum ($10^{-5}$ Torr) and vacuum+heat (400$^{o}$ C) had no effect on the value of friction coefficients. Since the surface of the specimens must have been very favorable to the occurrence of strong adhesion (i.e., in comparison to air and clean room conditions), it is reasonable to conclude that atomic interactions (i.e., adhesion) which occurred at the elastically deformed asperity junctions must have been insignificant. Therefore, one can conclude that plastic deformation, in the form of micro asperity deformation and sub-micron plowing, is the dominant mechanism in dry sliding of any crystalline solid.

The fact that all combinations involving silicon carbide resulted in the lowest mean friction coefficients suggests that in these combinations, the asperity contact stresses were lowest and hence the applied normal load was distributed more than in other test combinations. This also meant that with silicon carbide, a larger

portion of the real area of contact must have undergone elastic deformation and thus dissipated larger amounts of energy due to adhesional effect, in comparison to other test combinations. The remaining portion of the real area of contact, which underwent plastic deformation, must have been smaller and thus dissipated less energy in the form of dislocation generation and motion. Furthermore, since the effect of adhesion has been shown to be insignificant, the overall energy dissipation, hence friction, was smaller when silicon carbide was used as a base specimen. Using the same logic, the fact that all combinations involving silica glass resulted in the highest mean friction coefficients suggest that the asperity contact stresses and the portion of the real area of contact that underwent plastic deformation must have been the highest.

Another important conclusion is that if pure elastic deformation can be achieved at the sliding interface, then the resulting friction coefficient should be extremely small. This is because atomic interactions (i.e., adhesion) at elastically deforming asperity junctions have been shown to be negligible even when the circumstances needed for strong adhesion were very favorable (friction coefficients in air, clean room, vacuum, and vacuum+heat were virtually equal). Therefore, in any engineering situation, the resulting friction coefficient should be extremely small when only pure elastic deformation (i.e., no viscoelastic or anelastic deformation) is involved in sliding.

## 2.6 References


1. Kim, D. E., "Investigation of the Microscopic Mechanisms of Friction," Ph.D. Thesis, Department of Mechanical Engineering, M.I.T., May 1991, pp. 95-126.

2. Sherwood, R.G., "Gases and Vapors from Glass," *J. American Chemical Society*, Vol. 12, No. 6, 1918, pp. 448-458.

3. Harris, J.E., and Schumacher, E.E., "Measurements on the Gases of Known Chemical Compositions," *J. Ind. Eng. Chem.*, Vol. 15, No. 2, 1923, pp. 174-177.

4. Holland, L., The Properties of Glass Surfaces, Chapman and Hall, London, 1964, pp. 212-218.

5. Wagner, C., "Passivity during the Oxidation of Silicon at Elevated Temperatures," *J. of Applied Physics*, Vol. 29, No. 9, pp. 1295-1297.

6. Yabumoto, N., Minegishi, K., Saito, K., Morita, M., and Ohmi, T., "An Analysis for Cleaned Silicon Surface with Thermal Desorption Spectroscopy," in Proceedings of the First International Symposium on Cleaning Technology in Semiconductor Device Manufacturing, Hollywood, Florida, 1989, pp. 265-272.

7. Kaplan, R., and Perill, T.M., "Reduction of SiC Surface Oxide by a Ga Molecular Beam: LEED and Electron Spectroscopy Studies", Surface Science Letters, v. 165., 1986 pp. L45-L52.

# Appendix I: Analysis of Conditions Necessary for Removal of Adsorbed Gases from the Surface of Solids

## 1 Surface of solids

When a crystal is cleaved, the atoms on the surface have fewer neighboring atoms (fewer bonds) and higher energy levels than the atoms in the bulk of the solid. As a result, there is a "drive" to decrease the difference in the free energy (surface energy) between them, and this "drive" is the fundamental explanation for all surface phenomena. The surface energy of a solid can be reduced by either decreasing the surface area (by adhesion to another surface) or by lowering the energy of an individual surface atoms (by adsorption or by surface rearrangement).

## 2 Adsorption

Since this is a very complicated subject by itself, only the most relevant topics will be discussed here. In general, adsorption can be divided into two classes: physical adsorption and chemisorption. Physical adsorption takes place in seconds or in minutes and occurs as result of a nonspecific attraction (i.e., van der Waals forces) between the solid and the adsorbate. This is a reversible process and the adsorbate may be removed by simply lowering the pressure of the system. Chemisorption, on the contrary, may be rapid or slow and may occur above or below the critical temperature of the adsorbate. It is distinguished from physical adsorption in that some degree of specific chemical interaction between the adsorbate and the adsorbent is involved, and correspondingly, the energies of adsorption may be quite large and comparable to those of chemical bond formation. A gas that is chemisorbed on a surface may be difficult to remove by merely reducing the pressure. Although the extremes are easily distinguishable, there is no sharp dividing line between these two types of adsorption, .

A chemically adsorbed layer is usually only one molecule in thickness. Physically adsorbed molecules, however, depending on the partial pressure of the gas, can have substantial thickness. At very low partial pressures, adsorption is typically a monolayer in thickness, but as the partial pressure approaches the saturation pressure of the gas, multilayers can build up by bulk condensation.

An approach that was used for this investigation was to study adsorption from the point of view of adsorption time. Consider a molecule in the gas phase which is approaching the surface of the solid. If there were absolutely no attractive forces between the molecule and the solid, then the time of adsorption of the molecule in the vicinity of the surface would be on the order of molecular vibration time, or about $10^{-13}$ sec., and there would be no exchange of energy between the molecule and the solid. If however, there were some attractive forces present, then the average time of adsorption, $\tau$, of the molecule on the surface is given by [I-1]:

$$\tau = \tau_o \exp^{(Q/RT)} \text{ (sec)} \qquad \text{(I-1)}$$

where $\tau_o \cong 10^{-13}$ sec (time for specular reflection); R = gas constant = 8.28 J/mole $^oK$; T = absolute temperature; Q = energy of adsorption.

In addition to Q and $\tau$, another quantity of interest is the surface concentration $\Gamma$, where

$$\Gamma = Z\,\tau \quad \text{(mole/ cm}^2\text{)} \qquad \text{(I-2)}$$

and Z, the number of moles colliding per square centimeter per second is given by:

$$Z = 0.23\ P\ (3/MRT)^{2/3} \qquad \text{(I-3)}$$

In order to prevent an appreciable amount of adsorption on a surface, the time of adsorption must be very small compared to the time required for a new molecule to arrive at a given site. The time of adsorption was calculated previously by Bromwell [I-2] for several assumed values of adsorption energy and is shown in Table I-1.

At a very low value of Q, $\Gamma$ as given by equation I-2 is of the order expected on the basis that the gas phase continues uniformly just up to the surface, so that the net surface concentration is essentially zero. With intermediate values of Q (few kJ/mole), $\Gamma$ has increased considerably, and its value may be comparable to that for a complete monolayer. Thus, if Q is 37.6 kJ/mole, then $\Gamma$ is about $10^{-8}$ moles/cm$^2$ for a gas at 25° C, 0.1 atmospheric pressure, and of molecular weight of 20; this just about corresponds to a complete monolayer. Qualitatively, this intermediate region corresponds to that of physical adsorption. The third region is one for which Q value are of the order of chemical bond energies, so that the adsorption process presumably involves chemical bond formation. The values of $\tau$ become quite large, indicating that the approach to equilibrium may be slow, and the $\Gamma$ values computed from equation I-2 become far greater than those corresponding to a monolayer. Such values are evidently meaningless and equation I-1 should be replaced by a more exact probability model [I-3]; this has been done by Langmuir and by many other workers since.

Table I-1: Adsorption Time for Several Adsorption Energies

| T<br>K | Q<br>kJ/mole | $\tau$<br>sec | Remarks |
|---|---|---|---|
| 300 | 0.4 | 1 x 10-13 | Essentially no adsorption |
| 300 | 9.5 | 1 x 10-12 | Region of physical adsorption |
| 300 | 21 | 4 x 10-10 | |
| 300 | 42 | 2 x 10-6 | Limit of chemisorption |
| 300 | 84 | 5 x 10+1 | Region of chemisorption |
| 600 | 84 | 2 x 10-6 | As temperature increases, time of adhesion decreases |
| 300 | 125 | 1 x 10+9 | 300 years |
| 300 | 420 | 1 x 10+150 | |

Due to the very complicated nature of the adsorption process, it is currently impossible, although very tempting, to assign a specific value to the adsorption energy. The "first" batch of molecules to impinge on a freshly cut surface will have a tendency to adsorb onto the most active sites such as edges, corners, and peaks of the asperities; this process corresponds to a large energy of adsorption. When these active sites are filled, adsorption takes place on less active sites and the corresponding adsorption energy decreases. Eventually, as the number of adsorbed molecules continue to increase, they begin to interact with each other, leading to less favorable conditions for adsorption, and a further decrease in the adsorption energy. However, there are experimental methods for measuring a rough values of adsorption energy [I-4].

## 3 Desorption

Desorption of solids surfaces involves two steps; (1) Removing the initially adsorbed material; (2) Preventing readsorption from the gas phase. The process of removing the initially adsorbed gases involves both pressure and temperature such that the equilibrium constant for desorption $K_p$, is large. $K_p$ is determined from the following equation [I-2]:

$$- \Delta F = R\ T\ \ln K_p \qquad \text{(I-4)}$$

where $\Delta F$ is the free energy change for the adsorption process.

Due to the very complicated nature of the bonding which occurs for most adsorption processes, it is currently impossible to write a chemical equation which will permit accurate calculation of reaction constants. However, the conditions required to prevent readsorption on a clean surface can be approximately determined and this knowledge can be used as a guide for predicting desorption

conditions. An analysis of a such situation was done by Bromwell [I-2]. The results of her analysis indicate that a gas molecule which adsorbs on a solid surface at a temperature T ($^{o}$K) and pressure P (mm Hg) must have a minimum adsorption energy, Q (cal/mole) given by:

$$Q = 5.1\ T\ (\ 5 - \log_{10} P) \quad \text{(cal/mole)} \qquad \text{(I-5)}$$

This equation was shown to be very similar to the experimentally obtained equation of adsorption energy of various gases adsorbed on the surface of tungsten [I-4]. A plot of Q vs. T is shown in Figure I-1.

Figure I-1 can be used to approximate the conditions required to prepare and to maintain a clean surface. For example, molecules with adsorption energies larger than 20 kcal/mole (chemisorption) cannot be removed even at very low pressures ($10^{-6}$ torr) without using elevated temperatures. On the other hand, molecules with adsorption energies less than 15 kcal/mole (physical adsorption) will not adsorb on a surface at pressures of $10^{-4}$ torr, even at room temperature. Therefore, in order to prepare clean surfaces (no physical or chemical adsorption) for the vacuum experiments, both a high temperature ($\approx$ 250$^{o}$ C) and a low pressure ($\approx$ $10^{-5}$ Torr) seem necessary.

The surface atoms of a solid are normally "immobile". At a temperature T (T > 0.3 $T_{melt}$) some surface migration can occur. Near 0.5 $T_{melt}$ the rate of migration and diffusion rapidly increases, and sintering begins to occur [I-3]. Therefore, a material which must be heated above this temperature to desorb the surface may not have the same surface arrangement of atoms or surface energy as it would have at a lower temperature.

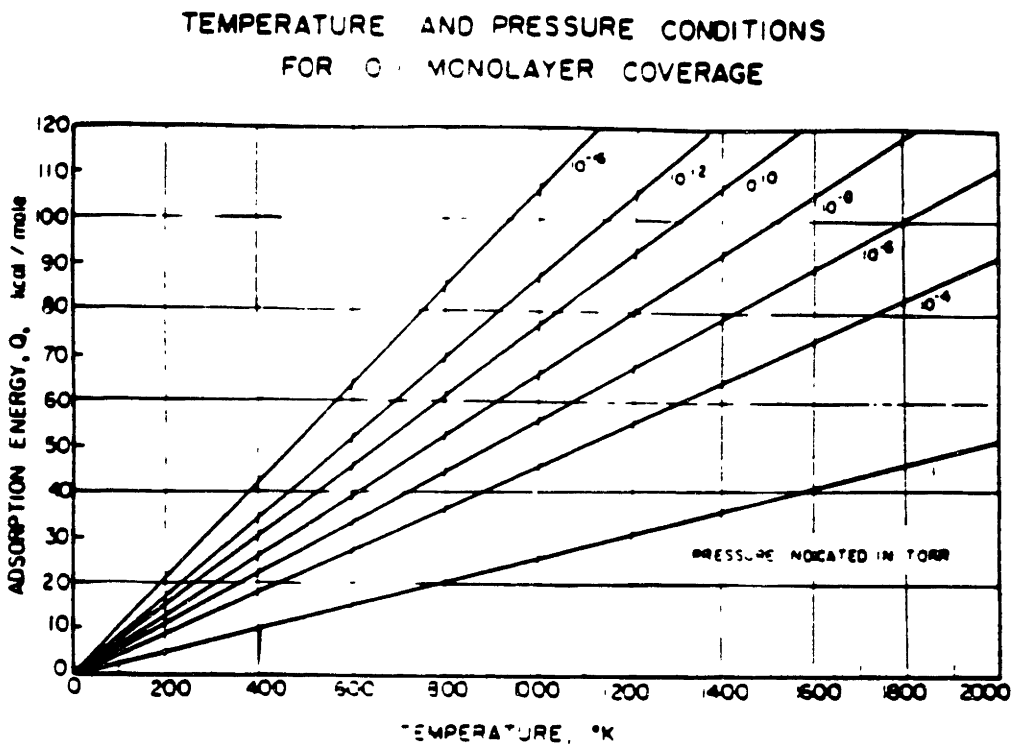


Figure I-1: Adsorption Energy vs. Temperature [I-2]

## Appendix I - References


I-1. Boer, J.H., The Dynamical Character of Adsorption, The Clarendon Press, Oxford, 1953, pp. 20-39.

I-2. Bromwell, L., Adsorption and friction Behavior of Minerals in Vacuum, U.S. Army Soil Mechanics Division Research Report R64-42, 1965, pp. 46-51.

I-3. Gregg, S.J., The Surface Chemistry of Solids, 2nd Edition, Reihold, N.Y., 1961, pp. 28-121.

I-4. Becker, J. A., "Study of Surfaces by Using New Tools", Solid State Physics, v. 7, Academic Press, New York, 1958, pp. 379-424.

# Chapter 3

# Elastomers

## 3.1 Introduction

To achieve minimum friction, the deformation that occurs at a sliding interface must be purely elastic, and any form of energy dissipation due to anelastic, viscoelastic, and plastic deformation at the sliding interface needs to be eliminated. Since this necessity has been shown to be very difficult to accomplish with crystalline solids (friction mechanisms dominated by plastic deformation), a covalently bonded and cross-linked elastic noncrystalline solid with the desired physical and chemical properties needs to be designed and produced so that only elastic deformation will occur at the sliding interface. The hypothesis for low friction and wear referred to in Chapter 2 was that resistance to crack nucleation and propagation could be achieved by confining the interaction at asperity contacts to smooth and hard elastomers that have desired elastic behavior. When these materials are so prepared as to have atomic scale or micron scale surface roughness, the energy dissipation should be extremely small. Since elastomers have traditionally been used as high friction materials, the degree of cross-linking is the key parameter that must be controlled in order to obtain the desired material properties (i.e., between viscoelastic and brittle material behavior) necessary for low friction.

The best candidate to test for low friction was Ebonite, a natural rubber mixed with a pre-determined amount of cross-linking agents; it is a heavily cross-linked elastomer with a frequency of cross-linking so high that the structure resembles a three-dimensional skeleton rather than a group of long-chain polymers which cross-link occasionally. As a consequence, Ebonite is a "hard,"

material whose mechanical characteristics of high strength and low extensibility represent the mechanical extremes of an elastomer.

## 3.2 The Dry Sliding Friction Mechanism of Rubber

In the past, research on the friction of rubber was mainly focused on the sliding or rolling of rubber on steel, glass, and concrete. The factors that influence rubber friction, unlike friction on metals, were found to be numerous: sliding speed, temperature, normal load, nominal area, inclusions in the rubber, surface roughness, and the properties of the elastomer. In the low-sliding speed regime, it was noted that the friction coefficient increased with increasing sliding speed until a maximum value of friction coefficient was reached. After that point the friction coefficient decreased even though the sliding speed was further increased [1] For a given sliding speed, the friction coefficient was found to increase initially with the sliding distance before reaching a steady state value.

Friction of elastomers has been explained in the past as consisting of two components: adhesion at the sliding interface (bonds are formed at the sliding interface and are then strained and broken when sliding occurs); and deformation due to delayed recovery of elastomers after indentation by a particular asperity [2-8]. Following the adhesion theory, many have advocated that in a normal sliding situation, the adhesion components exceed the deformation contribution; the high friction coefficients of the elastomers have been attributed to their high adhesive quality. However, in light of recent findings at M.I.T., such a statement may be proved to be incorrect; adhesion has been shown to be insignificant in many engineering situations, as discussed extensively in previous chapters.

## 3.3 Preparation of the Samples

For the experiments, natural rubbers were mixed with varying contents of sulfur (10 to 25 % by weight) in order to obtain the desired material properties necessary for low friction. The mixture was placed in a steel mold and pressed between two glass plates to form a cylindrical sulfur/rubber compound ( 2.5 cm in diameter and 0.95 cm in height), as shown in Figure 22. The glass plates were used to provide a smooth surface finish; polishing with abrasive papers was not done since polishing of sulfur/rubber compound results in the embedment of hard abrasive (alumina) on the surface of rubbers, which leads to destruction (i.e., energy dissipation by plastic deformation) of counter surface at the sliding interface (see Figure 23). The vulcanization was done at 135° C for twelve hours. The "hardness" of the sulfur/rubber compounds was measured with a *durometer,* and the result is shown in Figure 24. It should be noted that the hardness did not increase beyond 25% sulfur content, which was therefore the saturation point. The average surface roughness of the specimens was approximately 10 μm, as measured with the Dektek Surface Profilometer.

## 3.4 Experimental Procedure

The friction tests were conducted with a conventional reciprocating pin-on-disk apparatus, as shown in Figure 25. This apparatus was used under a Class 100 Clean-Room to minimize the possibility of particle entrapment at the sliding interface. The sliding speed was 0.3 cm/s, and the track length was 1.5 cm. The applied normal loads were 20 and 50 mN, and the distance of slide of each load was 16.20 m. The "pin" was a glass ball of 4 mm in diameter, and the "disks" were the sulfur/rubber compounds. All experiments were conducted at approximately 25° C and at a relative humidity of approximately 30%. The specimens were degreased with freon prior to each test.

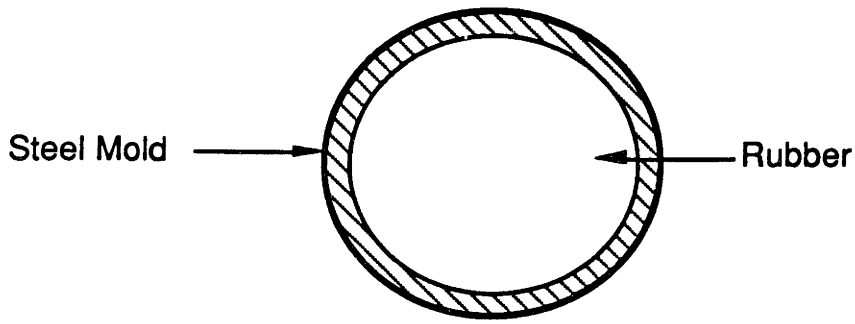


Figure 22: A schematic Drawing of a Sulfur/Rubber Specimen

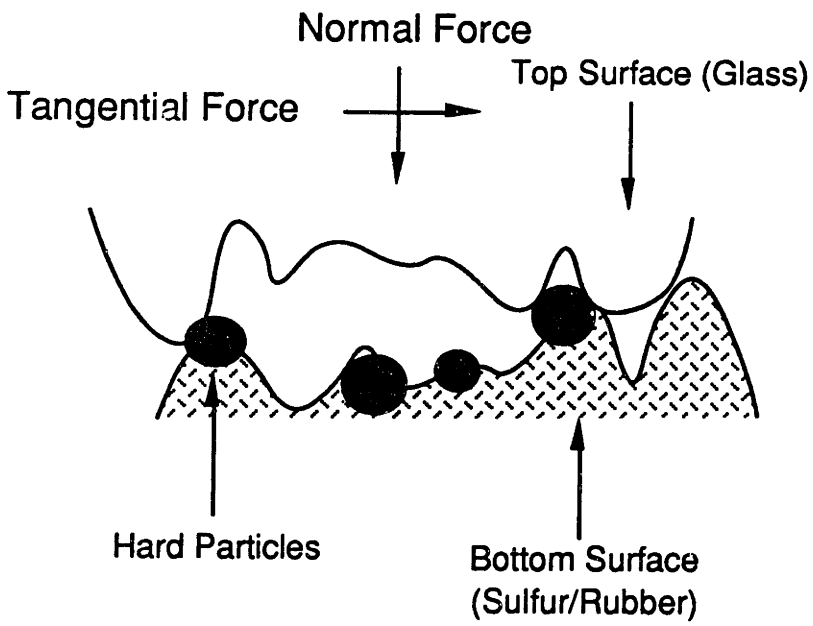


Figure 23: Destruction of Counter Surface by Hard Particles Embedded During Polishing of Sulfur/Rubber Compounds.

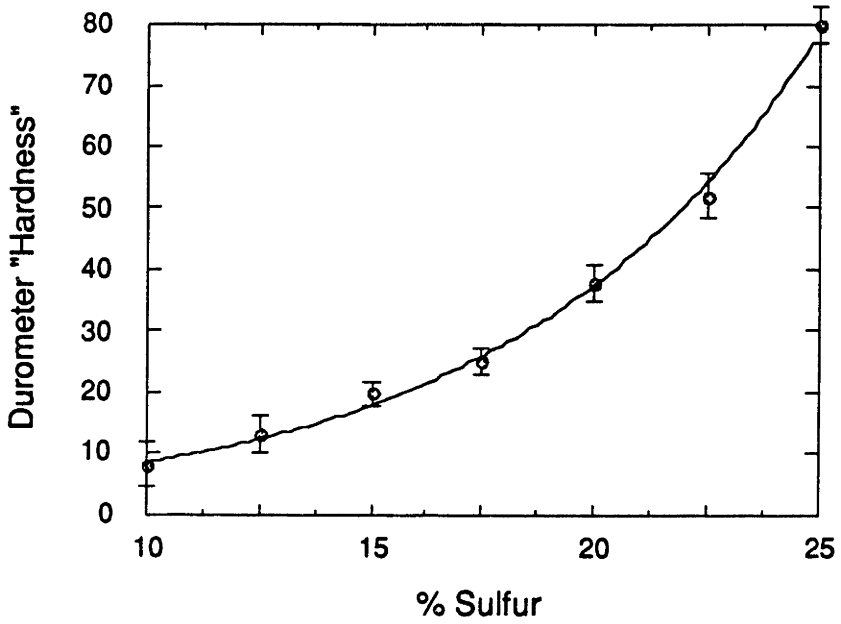


Figure 24: Durometer "Hardness" vs. % Sulfur.

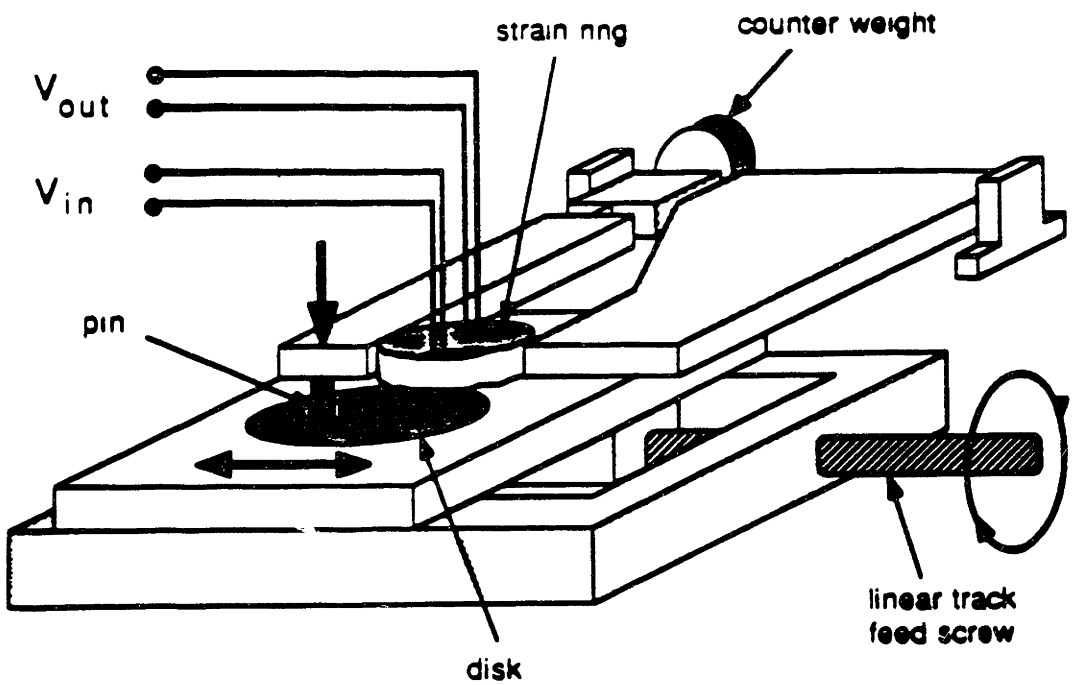


Figure 25: Reciprocating Friction Testing Apparatus.

## 3.5 Experimental Results

The experimental results show that the friction coefficient first decreased with increasing hardness until a minimum value ($\approx$ 0.3) was reached at 17.5% sulfur content (see Figure 26). The friction coefficient then slightly increased and eventually leveled off to about 0.5 as hardness was further increased. The values of friction coefficients varied from 1.9, at 12.5% sulfur content, to 0.5, at 25% sulfur content. The friction coefficients were independent of the applied normal loads used in this experiment. Surface damage was observed with SEM for all tests (see Figure 27). The surface of the wear track resembled a wave in the low-hardness regime, while the high-hardness regime showed surface cracks running perpendicular to the direction of the slide. It should also be noted that at the high hardness regime, the wear particles resembled a sheet-like shape. This observation will be discussed in more detail in the conclusion (see Figure 27-e). In the intermediate regime, surface damage was less visible.

## 3.6 Discussion and Conclusions

There are few possible modes of surface and subsurface crack nucleation, propagation and eventual failure. One possibility is for an asperity of the counter surface to mechanically anchor onto the asperity of the sulfur/rubber compound and "tear" the softer elastomer as shown in Figure 28. This seems to be the dominant mode of failure for the softer regime of the elastomer, as wave-like crests are observed on the wear tracks (see Figure 27-a). The viscoelastic behavior also contributes to the energy dissipation with the low modulus sulfur/rubber compounds.

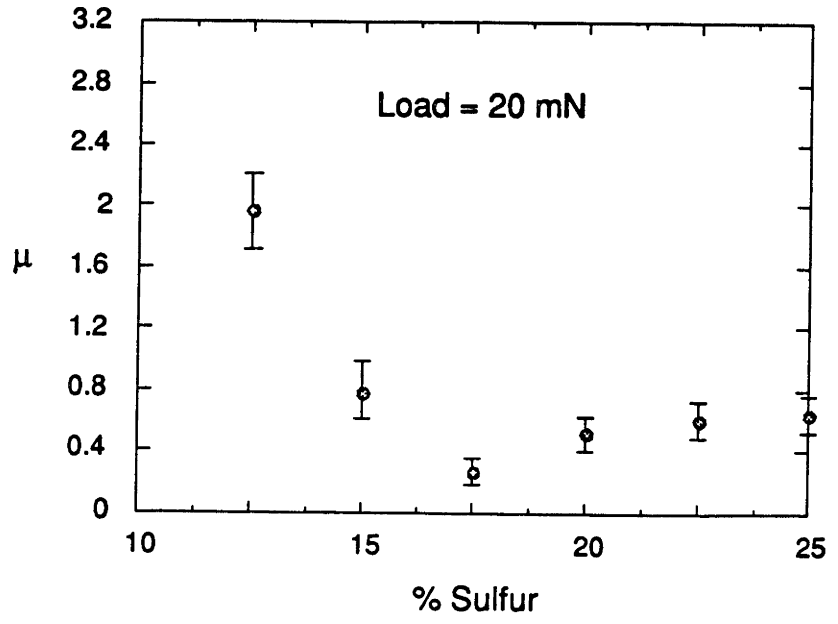


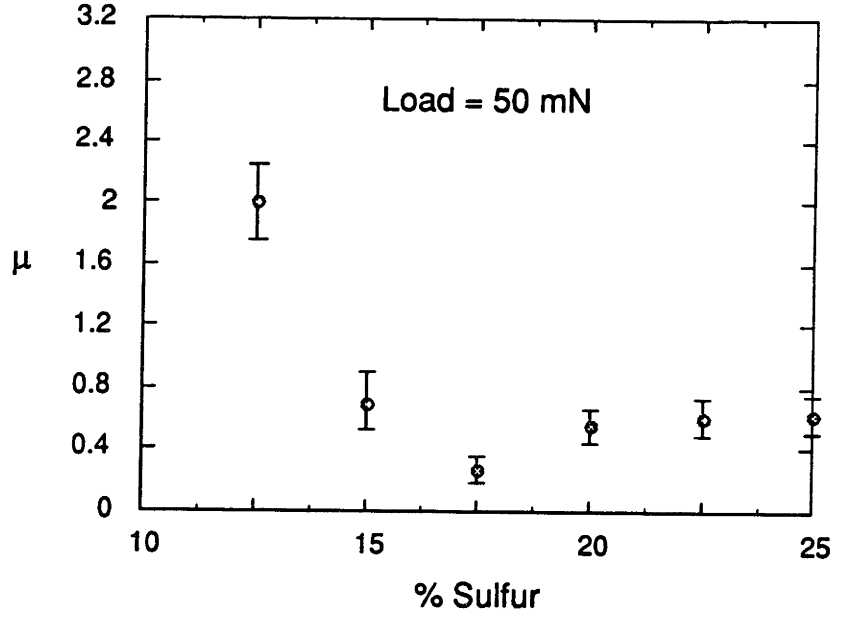


Figure 26: Steady State Friction Coefficient vs. % Sulfur: 20 and 50 mN Loads.

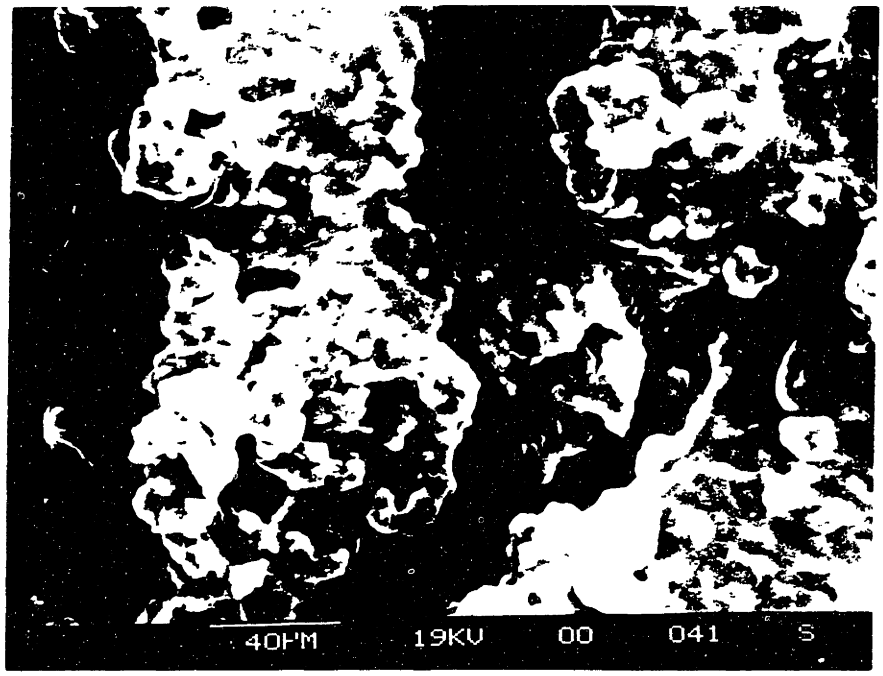


(a)

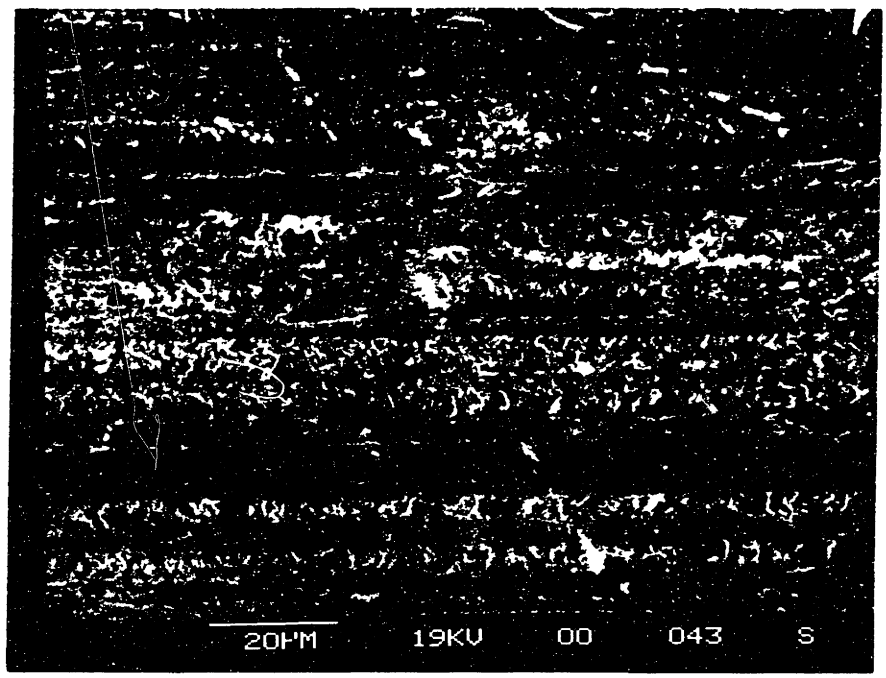


(b)

Figure 27: SEM photographs of the Wear Tracks of Sulfur/Rubber, 50 mN: (a) 12.5%S, (b) 15%S.

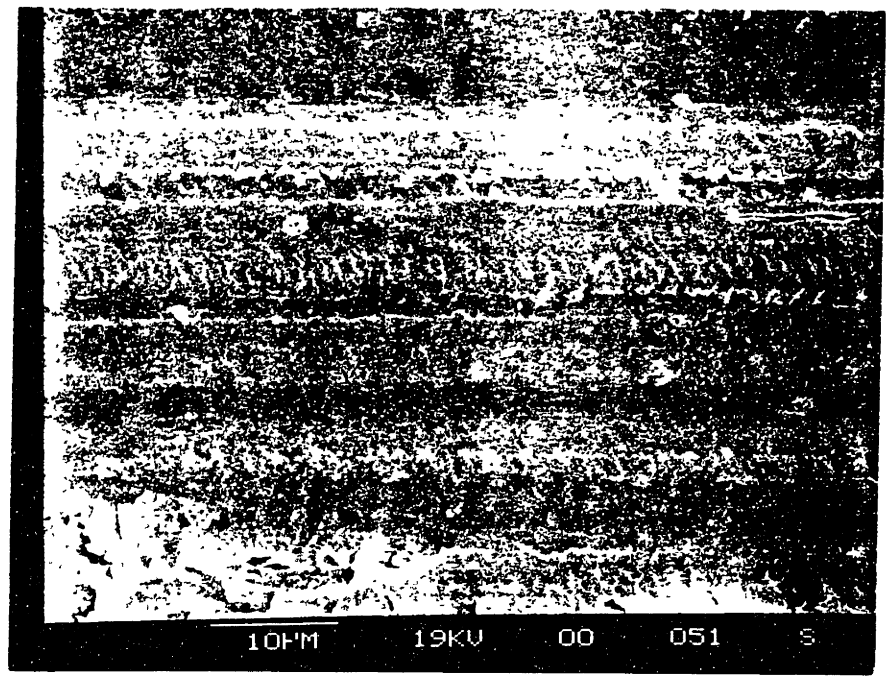


(c)

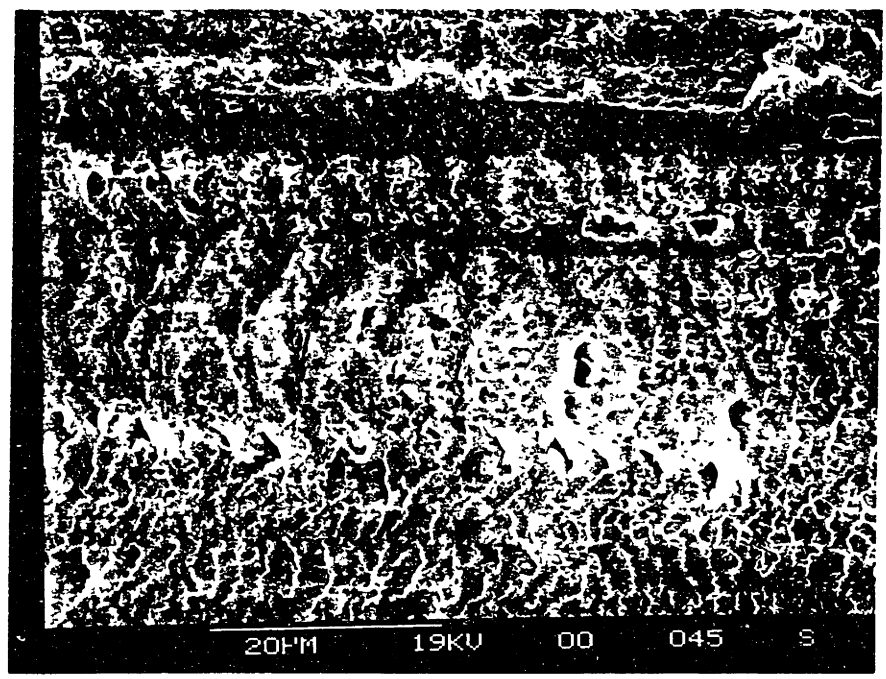


(d)

Figure 27: SEM photographs of the Wear Tracks of Sulfur/Rubber, 50 mN: (c) 17.5%S, (d) 20%S.

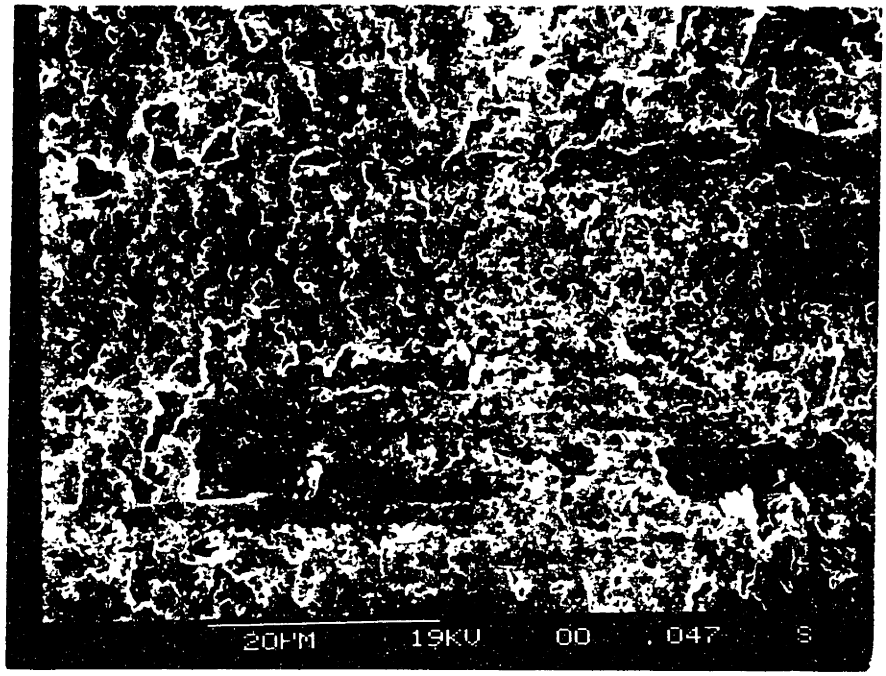


(e)

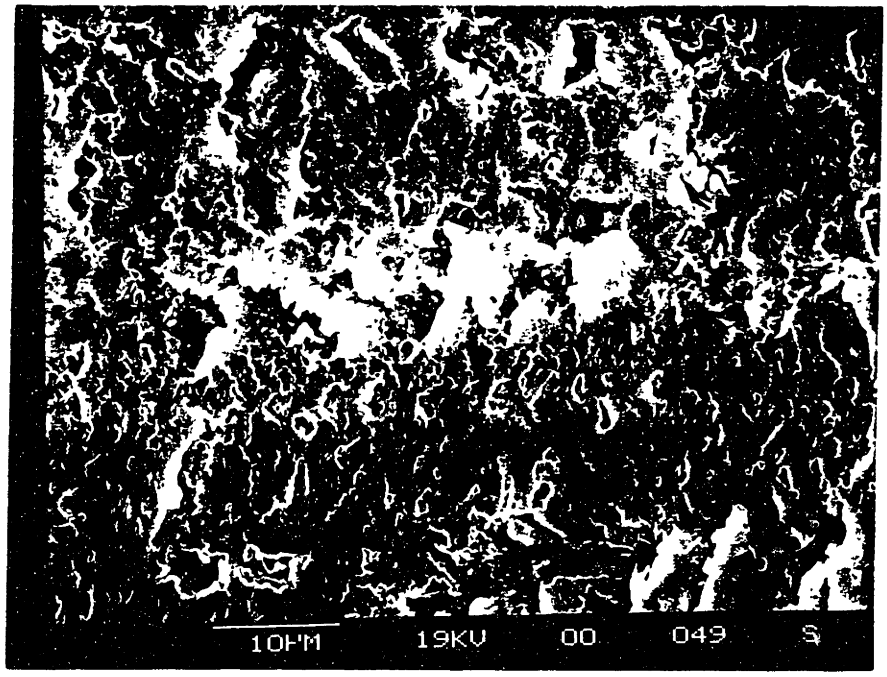


(f)

Figure 27: SEM photographs of the Wear Tracks of Sulfur/Rubber, 50 mN: (e) 22.5%S, (f) 25%S.

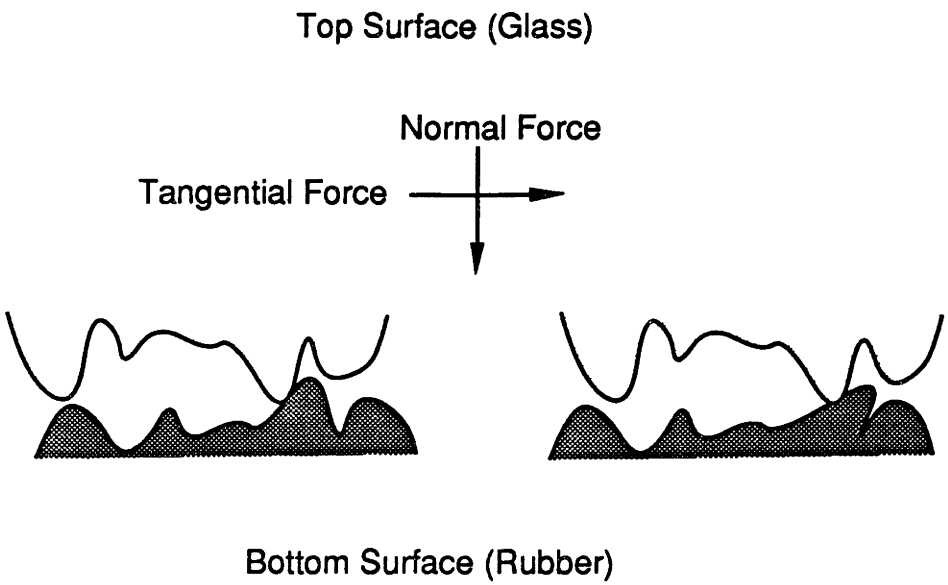


Figure 28: One Possible Surface Damage Mode

Another possible failure mode for the elastomer is that, like glassy polymers, cracks can initiate at the surface right behind the slider when the asperity contacts are blunt, or at the tip of sharp asperities, and propagate radially at the surface, axially into the surface from the asperity tip, and laterally at the subsurface [7] (see Figure 29). The final possibility is that the cracks can form at the subsurface due to the delamination and fracture resulting from the bulk deformation of the surface; it should be noted that the wear particles resemble a "sheet" in this situation [9]. For sulfur/rubber compounds of high modulus (i.e., high sulfur content) the fracture most likely starts from the surface, since surface defects are commonly present, but the subsurface fracture also must have occurred as seen from the sheet-like wear particles on the wear tracks (see Figure 27-f). In either mode, the plastic deformation seems to be the dominant mechanism with the high modulus sulfur/rubber compounds. The sulfur/rubber compounds of medium modulus (intermediate sulfur content), although they decreased both the viscoelastic and plastic deformation, most likely still underwent a small amount of all three possible failure modes.

From the experimental results it appears that the minimum friction cannot be achieved by controlling the hardness alone. Although a low value of friction coefficient was obtained in between the extremes of the mechanical behaviors (viscoelastic and brittle behavior), it was nevertheless impossible to totally eliminate the plastic and viscoelastic deformation. Elastomers, depending on the degree of crosslinking, always seemed to exhibit significant amounts of energy dissipation due to anelastic and viscoelastic effects or plastic deformation at asperity junctions. Even in the absence of plastic deformation, the elastomers, due to high subsurface stresses, can still undergo large bulk deformation, which leads to significant energy dissipation through anelastic and viscoelastic effects (see Figure 30). Therefore, one must have a smooth and very thin elastic layer (at least in the order of surface roughness) on top of a hard substrate for the minimization of friction. In this case, the hard substrate can support the load as well as limiting bulk deformation

while the soft top layer, such as 17.5% sulfur content compound, can allow elastic deformation at the asperity junctions (see Figure 31).

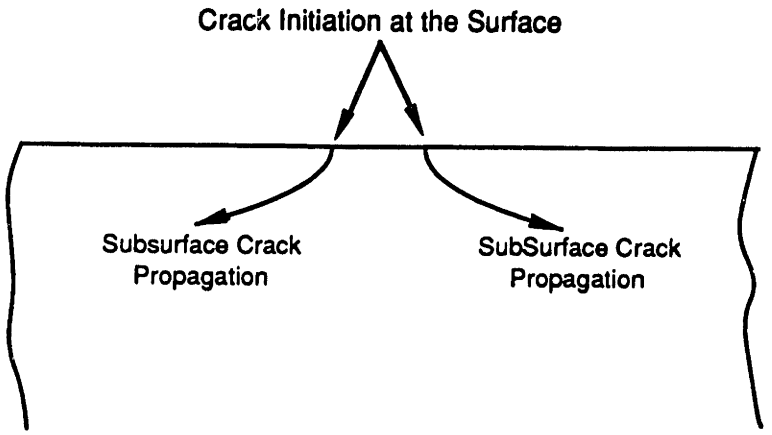


Figure 29: Cracks Initiating at the Surface.

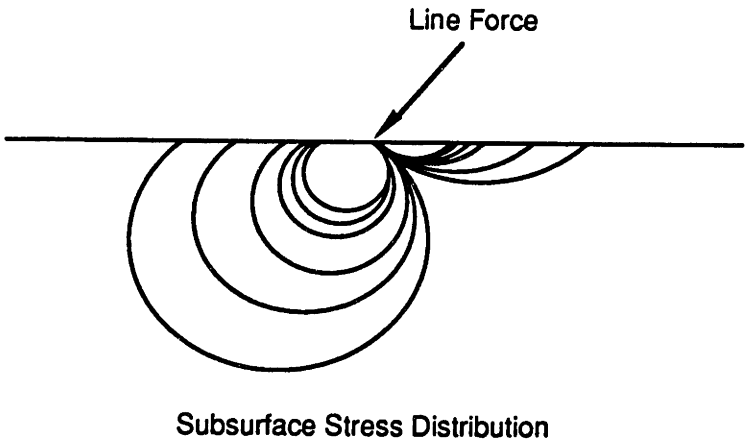


Figure 30: Theoretical Stress Distribution Produced by a Line Force on the Edge of a Semi-Infinite Elastic Plane; High Subsurface Stress Leading to Large Bulk Deformation

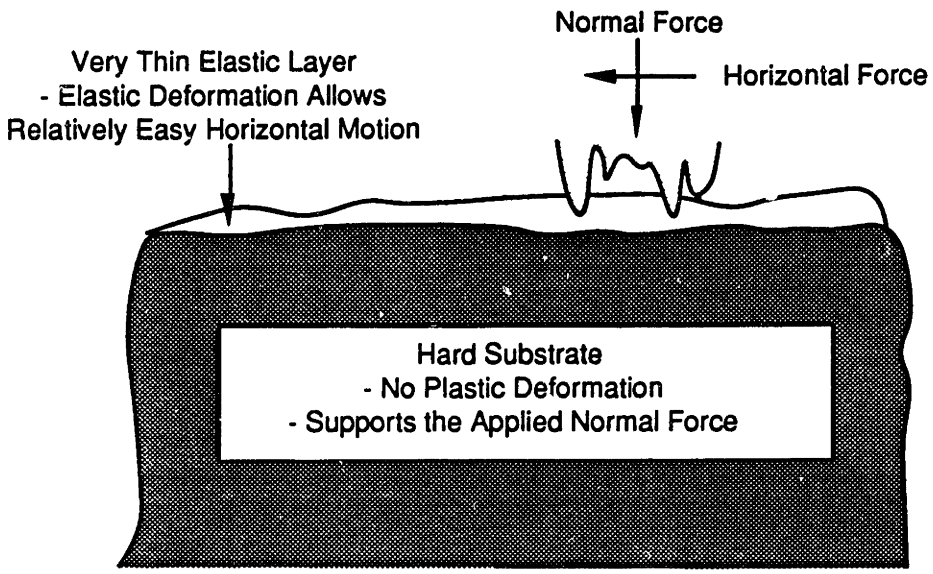


Figure 31: Very Thin Elastic Layer on Top of a Hard Substrate

## 3.7 References


1. Savkoor, A.R., "On the Friction of Rubber," *Wear*, Vol. 8, 1965, pp. 222-237.

2. Grosch, K.A., "The Relation Between the Friction and Viscoelastic Properties of Rubber," *Proc. Roy. Soc.*, A, Vol. 274, 1963, pp. 21-39.

3. Schallamach, A., "A Theory of Dynamic Rubber Friction," *Wear*, Vol. 6, 1963, pp. 375-382.

4. Moore, D.F., "A Review of Adhesion Theories for Elastomers," *Wear*, Vol. 22, 1972, pp. 113-141.

5. Moore, D.F., The Friction and Lubrication of Elastomers, Pergamon Press, 1972, pp. 193-195.

6. Savkoor, A.R., "Adhesion and Deformation Friction of Polymer on Hard Solids," Advances in Polymer Friction and Wear, Ed. Lee L.H., Plenum Press, 1974, pp. 71-121.

7. Fuller, K.N., and Tabor, D., "The Effect of Surface Roughness on the Adhesion of Elastic Solids," *Proc. R. Soc. Lond.*. A, Vol. 345, 1975, pp. 327-342.

8. Roberts, A.D., "Theories of Dry Rubber Friction," *Tribology International*, April 1976, pp. 75-81.

9. Suh, N.P., "The Delamination Theory of Wear," *Wear*, Vol. 25, 1973, pp. 111-124.

# Appendix I: Elastomers - Rubbers

## 1 Structures of Elastomers

Elastomeric behavior is exhibited by highly cross-linked long chain polymers. For such polymers to display rubber-like elasticity, the backbone of the chain must be very long and have many kinks and bends. The chain must also be cross-linked by primary chemical bonds at every several hundred atoms. In addition, the chains must be in constant motion; that is they must have considerable kinetic energy within the temperature range for which elastomeric behavior is manifested. The cross-linking can be provided by the addition of sulfur to the rubber, as in vulcanization.

## 2 Vulcanization of Rubbers

Vulcanization, the transformation of rubber from a predominantly plastic state into a predominantly elastic state, is the most important reaction of raw rubber. The chemical and physical changes brought about by vulcanization have made possible the enormous expansion in the commercial use of rubber. When natural rubber and sulfur are heated together, the vulcanization reaction yields a product which is much stronger, tougher, and less sensitive to temperature extremes than is the raw rubber.

### 2.1 Sulfur Used Alone

A predetermined amount of sulfur is incorporated into crude rubber by mastication. When the mixture, or "compound," is completely homogeneous, it is placed in a mold, which is heated under pressure, generally in a platten press. When the temperature rises above the melting point of sulfur (110 $^{o}$C), the sulfur becomes evenly diffused throughout the entire mass and is partially dissolved

in the rubber. The quantity of combined sulfur depends not only on the quantity of sulfur used in making the compound, but also on the temperature and period of heating.

There are different types of vulcanization products, and their properties vary with their combined sulfur content. Vulcanization, using up to 8 or 10 percent by weight of combined sulfur, gives soft rubber, which makes up most of commercial rubber products. Semihard rubbers contain 10 to 25 percent of combined sulfur. These products show lower tensile strength and elasticity than soft rubbers display. A combined sulfur consumption of 25 to 32 percent gives a hard, very tough, and substantially nonelastic product, which is called hard rubber or ebonite.

# Chapter 4

## 4.1 Conclusions

(1) Experiments have shown that plastic deformation, in the form of micro asperity deformation and sub-micron plowing, must have occurred in dry sliding of atomically smooth and hard crystalline solids. Even atomic scale roughness (0.1 nm) was large enough to cause mechanical interactions in the form of dislocation generation and motion. Furthermore, atomic interactions (i.e., adhesion) seem to be an insignificant contributor to friction; vacuum ($10^{-5}$ Torr) and vacuum+heat (400° C) had no effect on friction. Therefore, mechanical interactions must dominate friction in dry sliding of any crystalline solids.

(2) The experiments have also indicated that the minimum friction may be achieved by resisting crack nucleation and propagation, and by confining the interaction at asperity contacts to very smooth (i.e., atomic or micron scale roughness) non-crystalline materials that have good elastic (i.e., no viscoelastic or anelastic) behavior. Furthermore, the elastic behavior should be confined to a very thin layer (i.e., on the order of surface roughness) on top of a hard substrate in order to minimize the energy dissipation due to unavoidable anelastic and viscoelastic effects.

(3) The piezoceramic tribological apparatus can measure small frictional forces between two sliding flat surfaces in contact.

## 4.2 Recommendations

(1) To design and produce a "material" with very smooth surface finish and very thin elastic layer on top of a hard substrate. This may be achieved by coating an atomically smooth and hard surface with a very thin layer of soft metals or non-crystalline materials.

(2) To design and produce a surface with a very thin layer of "whiskers". The whiskers should be fibers of either soft metals or polymers that are partially embedded in a hard substrate such that a "geometrical elasticity" can be provided for easy shearing at the contacting interface (see Figure 32). This surface may be economically produced by using either metallic or polymeric fibers to produce an eutectic composite silicon wafers through the Czochralski technique. With this technique, the fibers should be embedded parallel to each other in a single crystal silicon matrix. The whiskers can then be created on the surface by selectively etching away the silicon crystals to reveal the metallic or polymeric fibers. Furthermore, by controlling the depth of etching, one may obtain the optimum whisker height necessary for achieving the minimum friction.

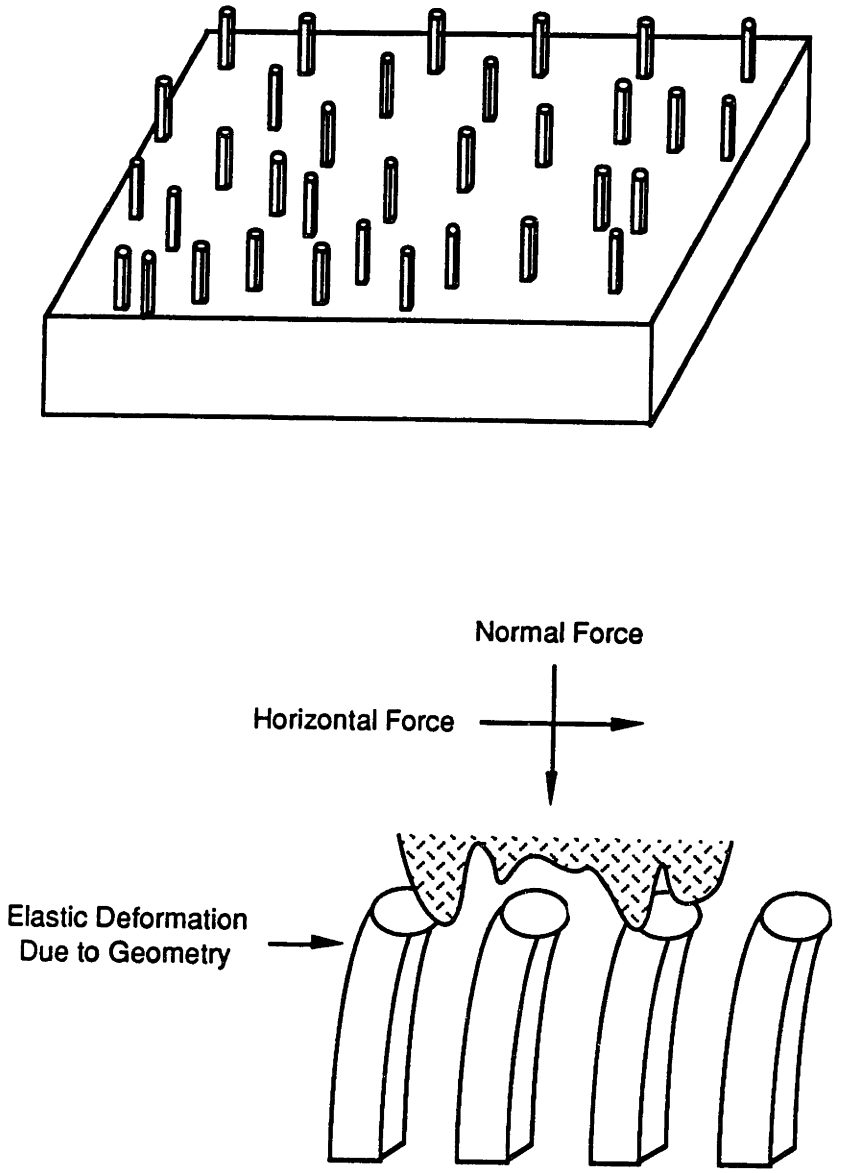


Figure 32: "Whiskers" on the Surface of a Solid